Paleoproductivity modes in central Mediterranean during MIS 20 - MIS 18: Calcareous plankton and alkenone variability

Patrizia Maiorano, Timothy Herbert, Maria Marino, Franck Bassinot, Pietro Bazzicalupo, Adele Bertini, Angela Girone, Sebastien Nomade, Neri Ciaranfi

Paleoceanography and Paleoclimatology

RESEARCH ARTICLE
10.1029/2021PA004259

Key Points:

- Coccolithophore and alkenones underline productivity changes in a reference Early/Middle Pleistocene record from the central Mediterranean
- Productivity proxies reflect millennial-scale climate changes with low/high values during cold and drier/warm and wetter conditions
- Similarity with the Dansgaard-Oeschger oscillations scenario suggests a common regional climate forcing over productivity through time

Supporting Information:

Supporting Information may be found in the online version of this article.

Correspondence to:

P. Maiorano,
patrizia.maiorano@uniba.it

Citation:

Maiorano, P., Herbert, T. D., Marino, M., Bassinot, F., Bazzicalupo, P., Bertini, A., et al. (2021). Paleoproductivity modes in central Mediterranean during MIS 20—MIS 18: Calcareous plankton and alkenone variability. *Paleoceanography and Paleoclimatology*, *36*, e2021PA004259. https://doi.org/10.1029/2021PA004259

Received 15 MAR 2021
Accepted 9 JUL 2021

Paleoproductivity Modes in Central Mediterranean During MIS 20—MIS 18: Calcareous Plankton and Alkenone Variability

Patrizia Maiorano[1], Timothy D. Herbert[2], Maria Marino[1], Franck Bassinot[3], Pietro Bazzicalupo[1], Adele Bertini[4], Angela Girone[1], Sebastien Nomade[3], and Neri Ciaranfi[1]

[1]Dipartimento di Scienze della Terra e Geoambientali, Università degli Studi di Bari Aldo Moro, Bari, Italy, [2]Department of Earth, Environmental, and Planetary Sciences, Institute at Brown for Environment & Society, Brown University, Providence, RI, USA, [3]Laboratoire des Sciences du Climat et de L'Environnement, CEA Saclay, UMR-8212, UVSQ, IPSL and Université Paris Saclay, Gif-Sur-Yvette, France, [4]Dipartimento di Scienze della Terra, Università degli Studi di Firenze, Firenze, Italy

Abstract Paleoproductivity is reconstructed across a Mediterranean benchmark record, the Early/Middle Pleistocene Montalbano Jonico section, cropping out in southern Italy. High-resolution coccolithophore and alkenone data (C_{37} and $C_{37:2}/C_{38:2}$ ratio) were collected in order to extend the data set on Mediterranean paleoproductivity pattern and forcing mechanisms. The multi-proxy record indicates low productivity during glacial and stadial phases and enhanced productivity during interglacial and interstadials. Increased surface water turbidity, cold-water temperature and polar-subpolar low salinity water incursion appear as the dominant controls for low productivity during Marine Isotope Stage (MIS) 20. Enhanced productivity during MIS 19c was sustained by warmer surface waters, coupled with a seasonal precipitation regime, providing higher nutrient availability. Productivity increases during interstadials with respect to stadials, in relation with enhanced land-derived nutrient input through river discharge during wetter winters. The productivity scenario we propose is similar to those reconstructed from deep-sea records in the central and western Mediterranean during Dansgaard-Oeschger oscillations over the last 70 ka. This indicates that similar forcing mechanisms acted on productivity dynamics on a regional scale over different times. We suggest that migration of the westerly wind system over the Mediterranean and the polar water inflow influenced productivity on a regional scale. The acquired data set provides new evidences on the environmental significance of the $C_{37:2}/C_{38:2}$ ratio and on its relation with surface water productivity.

Plain Language Summary Coccolithophores are calcifying unicellular algae and one of the most important marine phytoplankton group. In the present-day oceans their distribution strongly depends on environmental factors such as nutrient concentration, surface water temperature, sunlight availability. Therefore, changes in fossil coccolithophore assemblages are successfully used for paleoclimatic and paleoceanographic reconstructions. They are also the source of organic compounds (the alkenones), which provide estimation of paleotemperature and paleoproductivity. We used variations of coccolithophore assemblages and of alkenones to identify paleoproductivity variations in the central Mediterranean, in a nearshore environment, during a key Quaternary paleoclimate interval. Our approach benefited of other paleoenvironmental indicators such as sea surface temperature and stable oxygen and carbon isotopes available at the studied section. We find that past climate changes clearly affected coccolithophore productivity at our site. Paleoproductivity was clearly favored by warm surface waters and by seasonal nutrient availability resulting by enhanced humidity over the central Mediterranean region. Our data also provide new indications on the relation between coccolithophore assemblage and alkenone variations through climate phases which may have future implication on their use for paleoenvironmental reconstruction.

1. Introduction

Coccolithophores are a major component of oceanic phytoplankton and provide useful indications on surface water mass dynamics and particularly on primary productivity variations as well as on the relationships

between biology and oceanography (Baumann et al., 2005; Brand, 1994; Flores et al., 2003; Incarbona et al., 2013; Rickaby et al., 2010). Several sedimentary proxies are commonly used to estimate past changes in coccolithophore productivity, such as (a) variations in their absolute abundance, that is, number of coccoliths $\times$ g^{-1} of sediments (Ausín, Flores, Sierro, Bárcena, et al., 2015; Baumann & Freitag, 2004; Colmenero-Hidalgo et al., 2004; Martinez-Sanchez et al., 2019; Stolz & Baumann, 2010), (b) changes in their accumulation rate, that is, coccoliths $\times$ cm^{-2} $\times$ kyr^{-1} (Amore et al., 2012; Baumann et al., 2004; López-Otálvaro et al., 2009; Marino et al., 2014; Saavedra Pellitero et al., 2011; Steinmetz, 1994), (c) abundance of organic biomarkers produced by coccolithophores and preserved into the sediments, such as alkenones (Athanasiou et al., 2017; Emanuele et al., 2015; Quivelli et al., 2020; Sicre et al., 2000; Villanueva et al., 2001), or (d) the Sr/Ca ratio measured in the coccolith fraction (Cavaleiro et al., 2018; Mejía et al., 2014; Saavedra-Pellitero et al., 2017; Tangunan et al., 2017). The land-locked, semi-enclosed Mediterranean basin is highly sensitive to climate changes and therefore is an ideal natural laboratory for deciphering past sea-surface hydrological and productivity signals and identifying forcing mechanisms. The basin has undergone phases of enhanced surface water stratification and primary productivity events during periods of critical climate threshold, like intense humid climate conditions over the eastern Mediterranean related to minimal precession/maximal insolation (Hilgen, 1991; Lourens, 2004; Rossignol-Strick, 1985). This climate frame promoted the accumulation and preservation of organic matter at the sea floor and the formation of sapropels (e.g., Melki et al., 2009; Rohling et al., 2002, 2015; Rossignol-Strick et al., 1982; Toucanne et al., 2015). An extensive literature dealt with paleoproductivity variations associated with restricted interval of sapropel deposition in the Mediterranean, but only a few studies have focused on coccolithophore paleoproductivity over longer time windows including millennial scale climate oscillations within the Quaternary and impacting surface waters and therefore overall productivity. The available data mainly concern deep-sea records and are focused on the last glacial period, the last deglaciation and the Holocene, with a special focus to certain areas, that is, the Alboran Sea (Ausín, Flores, Sierro, Bárcena, et al., 2015; Ausín, Flores, Sierro, Cacho, et al., 2015; Bazzicalupo et al., 2020; Cacho et al., 2000, 2002; Colmenero-Hidalgo et al., 2004; Moreno et al., 2004, 2005) and the Sicily Channel (Incarbona, Di Stefano, et al., 2010; Incarbona, Martrat, et al., 2010; Incarbona et al., 2008, 2013; Sprovieri et al., 2003, 2006). The large multiproxy micropaleontological and geochemical data set available in the Alboran Sea provides a clear low/high productivity scenario matching Stadial/Interstadial phases during the Dansgaard-Oeschger oscillations (D-O) of the last glacial period, essentially related to the position and intensity of the north-westerly winds, affecting the inflow jet of Atlantic water and/or nutrient supply by climate-induced river runoff variability (Bazzicalupo et al., 2020; Cacho et al., 2000; Colmenero-Hidalgo et al., 2004; Moreno et al., 2005). The strong vertical density gradient related to Atlantic water inflow has been also considered as a forcing mechanism in weakening the vertical convection of the water column and producing a negative effect on biological productivity, during stadial phases in the Sicily Channel and on a larger scale within the Mediterranean (Incarbona et al., 2013). For the central Mediterranean and excluding the Sicily Channel area, the currently available data set remains largely incomplete and high-resolution Early to Middle Pleistocene Mediterranean records are extremely rare.

Our study aims to fill the gap of knowledge that exists on the productivity variations during the Early/Middle Pleistocene period in the central Mediterranean region, focusing across the interval from the late Marine Isotope Stage (MIS) 20 to the MIS 18 glacial inception. This interval includes MIS 19, considered a close analog of the present interglacial (Pol et al., 2010; Tzedakis et al., 2012) and which revealed orbital and millennial-scale climate variability in marine (Emanuele et al., 2015; Ferretti et al., 2015; Maiorano et al., 2016; Marino et al., 2020; Nomade et al., 2019; Sánchez Gõni et al., 2016; Toti et al., 2020; Tzedakis et al., 2012), lacustrine (Giaccio et al., 2015; Mangili et al., 2007; Regattieri et al., 2019), and ice core (Pol et al., 2010) records. We have investigated the expounded marine Ideale section in southern Italy (Figures 1A–1C), which is part of the Montalbano Jonico sequence (MJS, southern Italy) encompassing MIS 37-MIS 16. This sequence represents a world-class reference marine record for the Early-Middle Pleistocene transition (Bertini et al., 2015; Ciaranfi et al., 2010; Maiorano et al., 2010, 2016; Marino et al., 2015, 2016; Nomade et al., 2019; Petrosino et al., 2015; Simon et al., 2017). Thanks to its high sedimentation rate and well-documented supra-regional/global climate signatures (Figure 1C), the MJS offers the opportunity to gather a high-resolution data set from a shelf-upper slope environment, in a well-constrained chronological framework that is unique for the marine environment for this time period.

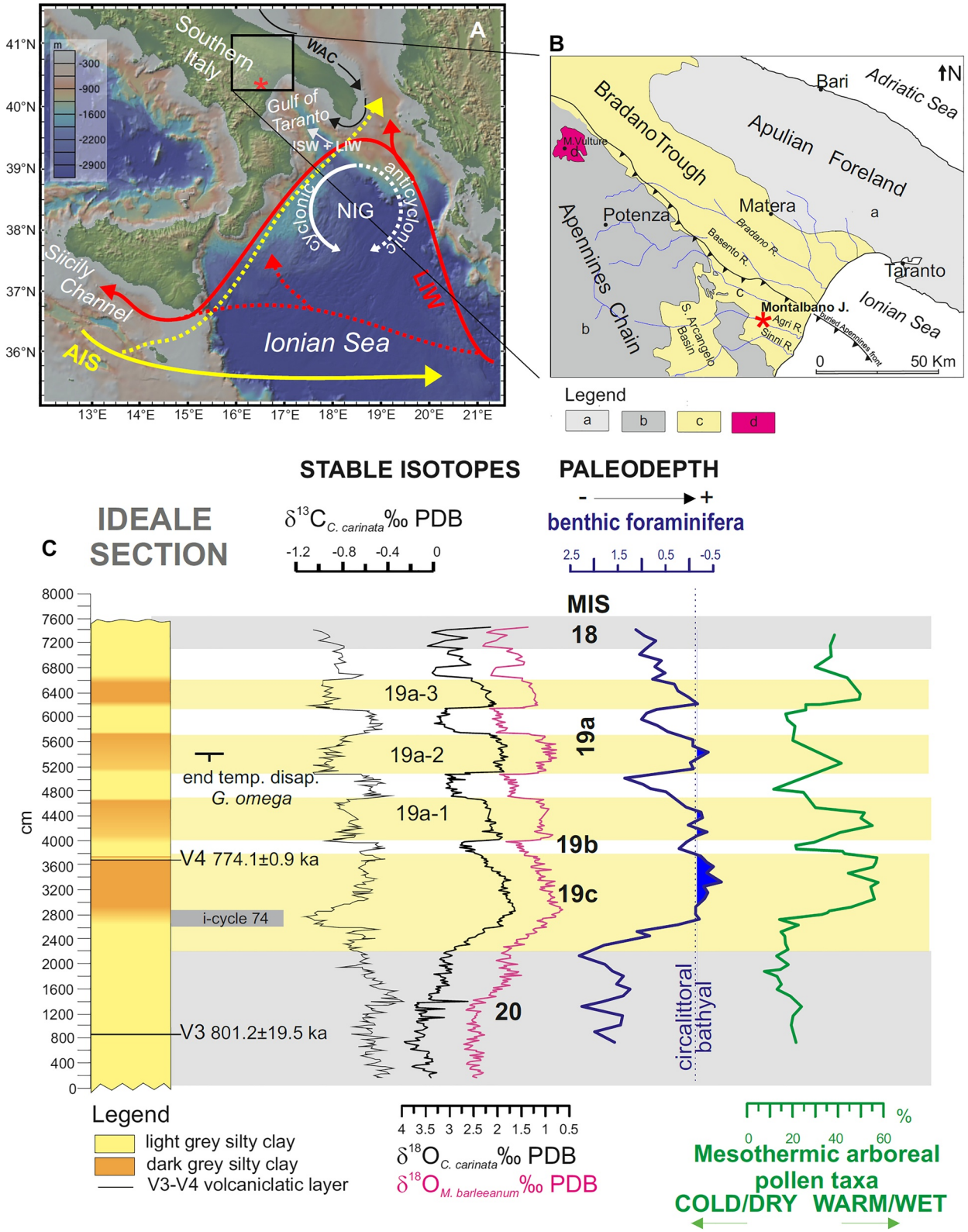
A
Southern Italy
WAC
Gulf of Taranto
ISW + LIW
cyclonic
anticyclonic
NIG
LIW
Sicily Channel
Ionian Sea
AIS
m
-300
-900
-1600
-2200
-2900
41°N
40°N
39°N
38°N
37°N
36°N
13°E
14°E
15°E
16°E
17°E
18°E
19°E
20°E
21°E
B
Bari
Adriatic Sea
N
Bradano Trough
Apulian Foreland
M.Vulture
Matera
Potenza
Bradano R.
Basento R.
Apennines Chain
Taranto
Ionian Sea
Montalbano J.
Agri R.
Sinni R.
S. Arcangelo Basin
Buried Apennines front
0
50 Km
Legend
a
b
c
d
STABLE ISOTOPES
PALEODEPTH
C
IDEALE SECTION
δ13C C. carinata ‰ PDB
-1.2 -0.8 -0.4 0
benthic foraminifera
- +
2.5 1.5 0.5 -0.5
MIS
18
19a-3
19a-2
19a-1
19a
19b
19c
20
end temp. disap.
G. omega
V4 774.1±0.9 ka
i-cycle 74
V3 801.2±19.5 ka
cm
8000
7600
7200
6800
6400
6000
5600
5200
4800
4400
4000
3600
3200
2800
2400
2000
1600
1200
800
400
0
circalittoral
bathyal
Legend
light grey silty clay
dark grey silty clay
V3-V4 volcaniclatic layer
4 3.5 3 2.5 2 1.5 1 0.5
δ18O C. carinata ‰ PDB
δ18O M. barleeanum ‰ PDB
%
0 20 40 60
Mesothermic arboreal pollen taxa
COLD/DRY WARM/WET

Figure 1.

It is important to mention here that data on paleoproductivity variation across the selected time interval are available only from the North Atlantic (Emanuele et al., 2015) and based on nannofossil accumulation rate variations. These data highlighted intra-interglacial high-frequency paleoproductivity variations related with the instability of mid-latitude North Atlantic sea surface hydrography.

Conscious that all paleoproductivity proxies suffer from ambiguities in interpretation, we take advantage of a multiproxy data set based on variations of total coccolithophore abundance (total N), total C_{37} alkenone concentration, $C_{37:2}/C_{38:2}$ ratio, distribution patterns of key coccolithophore taxa, in order to identify patterns consistent with climate-related paleoproductivity in the highly dynamic Mediterranean Sea. With the aim to identify forcing mechanisms in the study area, the data set is compared with the available multiproxy paleoclimate signals (Figure 1C), specifically with high-resolution oxygen and carbon stable isotope records (Nomade et al., 2019), alkenone-based sea surface temperature (SST) pattern and few planktonic foraminifera taxa (Marino et al., 2020) as well as pollen assemblage variations (Bertini et al., 2015; Maiorano et al., 2016).

2. Studied Area

2.1. Modern Oceanographic and Climate Setting

The studied marine sediments were deposited in the central Mediterranean, in the northern sector of the Ionian Sea and specifically in the paleo Gulf of Taranto (Figure 1A), an area very sensitive to record short-term climate variability even in the last millennia (e.g., Grauel et al., 2013; Taricco et al., 2015). The present-day surface circulation consists of the Western Adriatic Current (WAC) and the Ionian Surface Water (ISW). The WAC consists mostly of discharge from the Po River and northern Apennine rivers, thus representing a low-salinity and nutrient-rich coastal current, flowing in a narrow band from the northern Adriatic Sea into the Gulf of Taranto (Bignami et al., 2007; Poulain, 2001; Turchetto et al., 2007). Its stronger influence along the southern Italian coast and the Gulf of Taranto occurs during winter and spring (Milligan & Cattaneo, 2007; Poulain, 2001), while it is weaker during summer, due to the reduced river discharge. The WAC mixes with the warmer and more saline ISW, which enters the Gulf of Taranto from the central Ionian Sea (Figure 1A). Atlantic Water enters the Ionian Sea through the Atlantic Ionian Stream (AIS; Robinson et al., 1999) and flows along different pathways depending upon the decadal variability of the North Ionian Gyre (NIG; Figure 1A) and its cyclonic/anticyclonic circulation regime due to the interaction between the Adriatic and Ionian Seas (Civitarese et al., 2010; Gačić et al., 2010). At mid-water depth, between 200 and 600 m, the Levantine Intermediate Water (LIW) flows from the central Ionian Sea into the Gulf of Taranto (Malanotte-Rizzoli et al., 1997; Sellschopp & Álvarez, 2003). The deeper circulation of the Gulf of Taranto is associated with the Adriatic Deep Water (ADW), a dense water mass resulting from the deep convection active during late winter/early spring (Artegiani et al., 1997; Vilibić & Orlić, 2002).

The present-day Mediterranean climate is characterized by warm-dry summers and cool-wet winters, resulting from the seasonal shift of the subtropical high-pressure belt and the mid-latitude westerly system (Lionello, 2012; Lionello et al., 2006). Winter precipitations mainly derive from the southernmost location of the subtropical high, bringing rainy westerlies from the Atlantic Ocean over the Mediterranean. Summer dryness results from a prevailing anti-cyclonic atmospheric circulation over the Mediterranean, related to the northward displacement of the Hadley cell and of the Intertropical Convergence Zone (ITCZ).

Atmospheric and hydrographic conditions affect the Mediterranean trophic regime, which is among the poorest in the world's oceans (Béthoux et al., 1998) due to the semi-enclosed configuration and the anti-estuarine circulation pattern bringing nutrient depleted Atlantic waters into the basin. The nutrient

Figure 1. Location of the study area and stratigraphical/paleoclimate framework of the Ideale Section. The location of the Montalbano Jonico section is indicated by the red star. (A) Present-day sea surface and subsurface circulation in the Gulf of Taranto and Ionian Sea. AIS: Atlantic Ionian Stream; LIW: Levantine Intermediate Waters; WAC: Western Adriatic Current; ISW: Ionian Surface Water; NIG: North Ionian Gyre. Full/dashed lines denote different current pathways during cyclonic/anticyclonic regime. (B) Simplified regional geological setting of southern Italy. (a) Cretaceous Apulian Foreland units (b) Triassic-Neogene units of the Apennines Chain; (c) Plio-Pleistocene Apennines Foredeep units; (d) Quaternary volcanic units. (C): Lithological features and stratigraphical/chronological constraints of Ideale section from Ciaranfi et al. (2010), Maiorano et al. (2010) and Nomade et al. (2019). Benthic oxygen and carbon isotope data from Nomade et al. (2019); paleodepth profile from Stefanelli (2003); Mesothermic arboreal pollen taxa distribution from Bertini et al. (2015) and Nomade et al. (2019).

budget and phytoplankton biomass are related to seasonal modifications of the water column dynamics, that is, seasonal mixing providing injection of nutrients from deeper waters or, in specific areas, external nutrient being provided by river runoff and nutrient load from adjacent lands or atmospheric supply (e.g., D'Ortenzio & Ribera d'Alcalà, 2009; Ludwig et al., 2009; Richon et al., 2019). During summer, the density stratification inhibits the nutrients injection toward the surface layer, limiting autotrophic biomass. In late fall-winter, the upward mixing of underlying nutrients allows a slight but constant increase of biomass (e.g., Civitarese et al., 2010; Klein et al., 2003; Macias et al., 2015).

2.2. Stratigraphy and Paleoclimate Framework of the Ideale Section

The Ideale section (IS) deposited on the south-western margin of the Bradanic Trough (Casnedi, 1988), located between the Apennines Chain to the west and the Apulia foreland eastward (Figure 1B; 40°17′29.52″N, 16°33′10.58″E). The section is part of the Pleistocene Apennines Foreland unit. It is about 80 m thick, and consists of clays and silty-clays (Figure 1C) deposited in an upper circalittoral-upper bathyal setting (Ciaranfi & D'Alessandro, 2005; D'Alessandro et al., 2003; Stefanelli, 2003). Two volcaniclastic layers, V3 (at about 800 cm) and V4 (at about 3,620 cm), have been radiometrically dated and give $^{40}Ar/^{39}Ar$ ages of 801.2 ± 19.5 ka (Maiorano et al., 2010), and 773.9 ± 1.3 ka (Petrosino et al., 2015; 774.1 ± 0.9 ka, Nomade et al., 2019), respectively (Figure 1C). The very high resolution of recently generated benthic (*Cassidulina carinata* and *Melonis barleeanum*) $\delta^{18}O$ records allowed to obtain a precise stratigraphical and chronological framework for the IS which is described in detail in Nomade et al. (2019) and Simon et al. (2017), from MIS 20 to early MIS 18 (Figure 1C). The adopted age model includes both astronomical tie-points and dated tephra layers interbedded in the IS section, which represents the age-model strategy that better resolve the timing of MIS 19 (Nomade et al., 2019). The sedimentation rates are very high, ranging between 90 and 200 cm/ky (Nomade et al., 2019). The dark gray bands (Figure 1C), during interglacial MIS 19c and MIS 19a interstadials (19a-1, 19a-2, and 19a-3) correspond to dark silty-clays enriched in kaolinite and smectite content (Maiorano et al., 2016). They deposited during wetter conditions promoting chemical weathering on land and enhanced continental fresh water input (Bertini et al., 2015; Maiorano et al., 2016; Nomade et al., 2019). Conversely, the light gray bands are related to quartz and dolomite increases associated with enhanced supplies of the coarser grain size fraction supply during more arid climatic conditions (Bertini et al., 2015; Maiorano et al., 2016), from those rivers (Sinni, Agri, Cavone, Basento, and Bradano) representing the major tributary for the study area (Figure 1B). The dark and light intervals correspond to lower (interglacial, interstadials) and higher (glacial, stadials) benthic $\delta^{18}O$ values (Ciaranfi et al., 2010; Nomade et al., 2019), respectively, associated with higher (~180 m depth) and lower (~100 m depth) sea level (Aiello et al., 2015; Bertini et al., 2015; D'Alessandro et al., 2003; Marino et al., 2015; Stefanelli, 2003), suggesting a glacio-eustatic/climate control on sedimentary features of the IS. The lower values of benthic (*C. carinata*) $\delta^{13}C$ during full interglacial and interstadial phases have been interpreted as reflecting higher organic matter arrival/preservation at the sea bottom, likely in relation to higher primary productivity and water column stratification or organic matter influx from land (Marino et al., 2020; Nomade et al., 2019). The paleoenvironmental/paleoceanographic setting based on the $\delta^{13}C$ minima during the earliest MIS 19c (Nomade et al., 2019) together with co-registered micropaleontological evidences (Maiorano et al., 2016; Marino et al., 2020) support the interpretation of a sapropelic layer from 2,620 to 2,840 cm (Figure 1C) associated with insolation cycle 74 (i-c 74, 784 ka, Lourens, 2004; 785 ka, Konijnendijk et al., 2014).

3. Methods

3.1. Calcareous Plankton

One hundred sixty-six samples were investigated with a sample spacing of about 40 cm, providing a temporal resolution of ~200 years. Slides for coccolithophore analysis were prepared following Flores and Sierro (1997) to estimate absolute coccolith abundances (# coccoliths/g). Quantitative analyses were performed using a polarized light microscope at 1,000 × magnification. Abundances were determined by counting at least 500 coccoliths of all sizes. Reworked calcareous nannofossils, that is, taxa belonging to older (Mesozoic and Paleogene-Neogene) stratigraphic intervals, were estimated separately during this counting. Variations in the assemblage were assessed using percentages and number of coccoliths/g of

sediment. *Umbilicosphaera sibogae* s.l., *Calciosolenia* spp., *Discosphaera tubifera*, *Rhabdospaera clavigera*, *Umbellosphaera* spp., and *Oolithotus* spp., were here grouped as warm-water coccolith taxa (WWCT) according to their ecological preferences (Baumann et al., 2004; Boeckel & Baumann, 2004; McIntyre & Bé, 1967; Saavedra-Pellitero et al., 2010 Winter et al., 1994; Ziveri et al., 2004). The coccolith dissolution index (DI) was estimated using the method of Dittert et al. (1999) modified by Amore et al. (2012) according to the following ratio: DI = small *Gephyrocapsa*/(small *Gephyrocapsa* + *Calcidiscus leptoporus*). High values of DI indicate good preservation. Species dominance of the coccolithophore assemblage has been obtained using PAleontological STatistics Software 4.02 (Hammer et al., 2001) and is equivalent to 1-Simpson index. With regard to the taxonomy of gephyrocapsids, which are a major component of the assemblage, we followed the criteria adopted in Maiorano et al. (2013) separating small *Gephyrocapsa* < 3 μm, *Gephyrocapsa oceanica* > 3 μm with angle bridge > 50°, and *Gephyrocapsa caribbeanica* > 3 μm and closed central area. The identification of taxa other than gephyrocapsids refers to Jordan et al. (2004) and Young et al. (2003).

We also rely on the relative abundances of two key target planktonic foraminifera taxa, presented in more detail in a different study (Marino et al., 2020), that are, the herbivorous *Globigerina bulloides* and the polar-subpolar *Neogloboquadrina pachyderma* (sensu Darling et al., 2006). *Globigerina bulloides*, due to its opportunistic behavior (Schiebel & Hemleben, 2005; Schiebel et al., 1997), is used as an indicator of high nutrient content in surface water. In recent Mediterranean, *G. bulloides* is abundant during periods characterized by high productivity in surface waters related to upwelling, strong seasonal mixing (Bárcena et al., 2004; Hernández-Almeida et al., 2011; Mallo et al., 2017; Pujol & Vergnaud-Grazzini, 1995) or fertilization by river input (Rigual-Hernández et al., 2012) at the winter-early summer. The eutrophic affinity of *G. bulloides* in the fossil record has been also widely documented in different Mediterranean geological settings (e.g., Rohling et al., 1997 and references therein; Zachariasse et al., 1997; Kontakiotis, 2016 and references therein). *Neogloboquadrina pachyderma*, a polar-subpolar species (Darling et al., 2006; Hemleben et al., 1989) is used as a proxy of Atlantic cold (melt) water influx into Mediterranean (Bazzicalupo et al., 2018; Cacho et al., 1999; Capotondi et al., 2016; Girone et al., 2013; Marino et al., 2018, 2020; Pérez-Folgado et al., 2003; Sierro et al., 2005; Toti et al., 2020).

3.2. Alkenone Analysis

We analyzed 162 samples every 40–60 cm (average temporal resolution of ~200/300 years) in the same sediment layers sampled for calcareous plankton, stable isotopes and pollen. Alkenone extraction followed freeze-drying ~5 g of homogenized dry sediment, using 100% Dichloromethane (DCM) and a Dionex 200 Accelerated Solvent Extractor (ASE). Prior to quantification, extracts were evaporated with nitrogen and reconstituted with 200 μL of toluene spiked with n-hexatriacontane (C_{36}) and n-heptatriacontane (C_{37}) internal standards. Samples were purified by silica gel flash column chromatography to further isolate the ketone fraction. The silica gel was conditioned in glass pipettes with 6 ml of hexane, then eluted with 4 ml hexane, followed by 4 ml dichloromethane (ketone fraction). Alkenone concentrations ($C_{37:2}$, $C_{37:3}$, $C_{38:3}$ ethyl, $C_{38:3}$ methyl, $C_{38:2}$ 2ethyl, and $C_{38:2}$ methyl ketones, resolved to baseline under our chromatographic conditions) were determined using an Agilent Technologies 6890 gas chromatograph-flame ionization detector (GC-FID), with Agilent Technologies DB-1 column (60 m, 0.32 mm diameter, and 0.10 mm film thickness). Procedure entailed a 1-μl injection, initial temperature 90°C, increased to 255°C with 40°C/min rate, increased by 1°C/min to 300°C, increased by 10°C/min to 320°C, and an isothermal hold at 320°C for 11 min. The C_{37} total (ng/gram dry weight sediment) was derived by normalizing these areas to the peak areas of the internal C_{36} and C_{37} n-alkane standards and dividing by the weight of the sample extracted. Gas chromatography and column conditions were optimized to allow for accurate quantification of the four C_{38} alkenones (we found that daily trimming of the chromatographic column and regular maintenance of the GC inlet is essential to avoid "drift" in the column retention of C_{38} alkenones relative to the C_{37} alkenones). Long-term laboratory analytical error, estimated from replicate extractions and gas chromatographic analyses of a composite sediment standard is equivalent in temperature to ±0.1°C and to a relative error of 10% in quantifying C_{37}. The relative reproducibility of the C_{37}:C_{38} indices was approximately 3% (N = 12 replicates).

Alkenone paleothermometry relies on the temperature dependence of the degree of unsaturation (number of double bonds) observed in the suite of organic compounds ($C_{37:3}$ and $C_{37:2}$ alkenones) synthesized by marine surface-dwelling haptophyte algae (Marlowe et al., 1984; Prahl & Wakeham, 1987). There are several choices concerning which calibration to use to translate alkenone unsaturation ratio ($U^{k'}_{37}$) to SST (Conte et al., 2006; Müller et al., 1998; Prahl & Wakeham, 1987; Tierney & Tingley, 2018), but all give very similar estimates in the range of $U^{k'}_{37}$ encountered in the Ideale section. For this work, we used the Müller et al. (1998) calibration to translate $U^{k'}_{37}$ to SST. The whole alkenone-based SST record (Figure 2b) is already presented in Marino et al. (2020) and thus not introduced in the following result section. However, in Table S1, we also supply the Bayesian estimate and arguments (Text S1) for choosing the Müller et al. (1998) calibration.

4. Results

4.1. Calcareous Plankton

Total coccolithophore abundance (Total N) ranges between ~11×10^7 and ~102×10^7 (coccoliths/g; Figure 2c), with maximum values occurring during MIS 19c (783.7–773.1 ka). In contrast to their scanty present-day distribution in the Ionian Sea with respect to western Mediterranean (Knappertsbusch, 1993; Malinverno et al., 2003), gephyrocapsids represent the dominant taxa in the IS assemblage, with abundance ranging between 70% and 95% (Figure 2e), thus suggesting a different biogeography through time, although the rising of dominant *Emiliania huxleyi* among Noelaerhabdaceae lineage in the modern Mediterranean coccolithophore communities should be also considered. Small gephyrocapsids dominate during glacial MIS 20 and from MIS 19b upwards, with relative values ranging between 50% and 85%. Their lower abundances (~30%) characterize MIS 19c (~777–784 ka), while increases occur during interstadials MIS 19a-1 to 19a-3. Medium-sized gephyrocapsids (>3 μm), *G. caribbeanica* and *G. oceanica,* are rare (generally lower than 10%–15%) throughout the record, while noticeably relative abundance increase occurs during MIS 19c, reaching about 70% of the assemblage (Figure 2d). Among subordinate taxa, *Helicosphaera carteri* has percentage values no greater than ~7% (Figure 2f), with the highest abundance during MIS 20-earliest MIS 19c and at the onset of MIS 18. Minimum values are noticed during most of MIS 19c, between 783.7 and 773.1 ka. Distinct short-terms increases of *H. carteri* occur at the stadial phases of MIS 19a. *Florisphaera profunda* has a strongly fluctuating pattern (Figure 2g), with relative abundance generally not greater than 8% (occasionally reaching 11%) and the highest values during MIS 19c and at the base of MIS 19a-1. WWCT have rather low abundances (generally <1%) all through the section with the exclusion of a first slight increase at 784 ka and higher relative increase during the warm oscillation of MIS 19a-2 (Figure 2h). Reworked coccoliths reach 40% with respect to the indigenous taxa (Figure 2i), with the highest values during MIS 20 and earliest MIS 19 as well as distinct short-term increases tracing most of the stadial phases. The calcareous nannofossil dissolution index has values close to 1 through the entire section (Figure 3f), thus suggesting that dissolution was insignificant. Within the planktonic foraminifera assemblage *G. bulloides* is continuously present throughout the IS with several brief decreases/increases and a long-term increase from MIS 19b upwards (Figure 3h). *Neogloboquadrina pachyderma* occurs mainly during late MIS 20, with percentages never exceeding 5% of total assemblages (Figure 3i), and a brief incursion of the taxon is also recorded during the stadial part of MIS 19a-2. The coccolithophore data set is provided in Tables S2 and S3.

4.2. C_{37} Alkenone Concentration

Through the investigated interval, the total C_{37} alkenone concentration varies between 20 and 470 ng/gram (Figure 3d). The lowest values are recorded during MIS 20 and from 19a-2 upwards. An interval of marked increase is observed during most of MIS 19c, starting from about 784 ka, and sharp peaks also occur during 19b and 19a-1. The $C_{37:2}/C_{38:2}$ ratio has the lowest values (about 0.9) during MIS 20 (Figure 3b), while it reaches its maximum increase (about 1.1) during most of MIS 19c. Fluctuating values of the $C_{37:2}/C_{38:2}$ characterize the upper portion of the section, from MIS 19b upwards and showing increase/decrease during interstadials/stadials, with a prominent decrease at the cold oscillation between MIS 19a-2 and 19a-3 (Figure 3b). Note that both the C_{37} total and the $C_{37:2}/C_{38:2}$ ratio rather strongly mirror changes in the total coccolith abundance (Figure 3e). Alkenone concentrations are provided in Table S4.

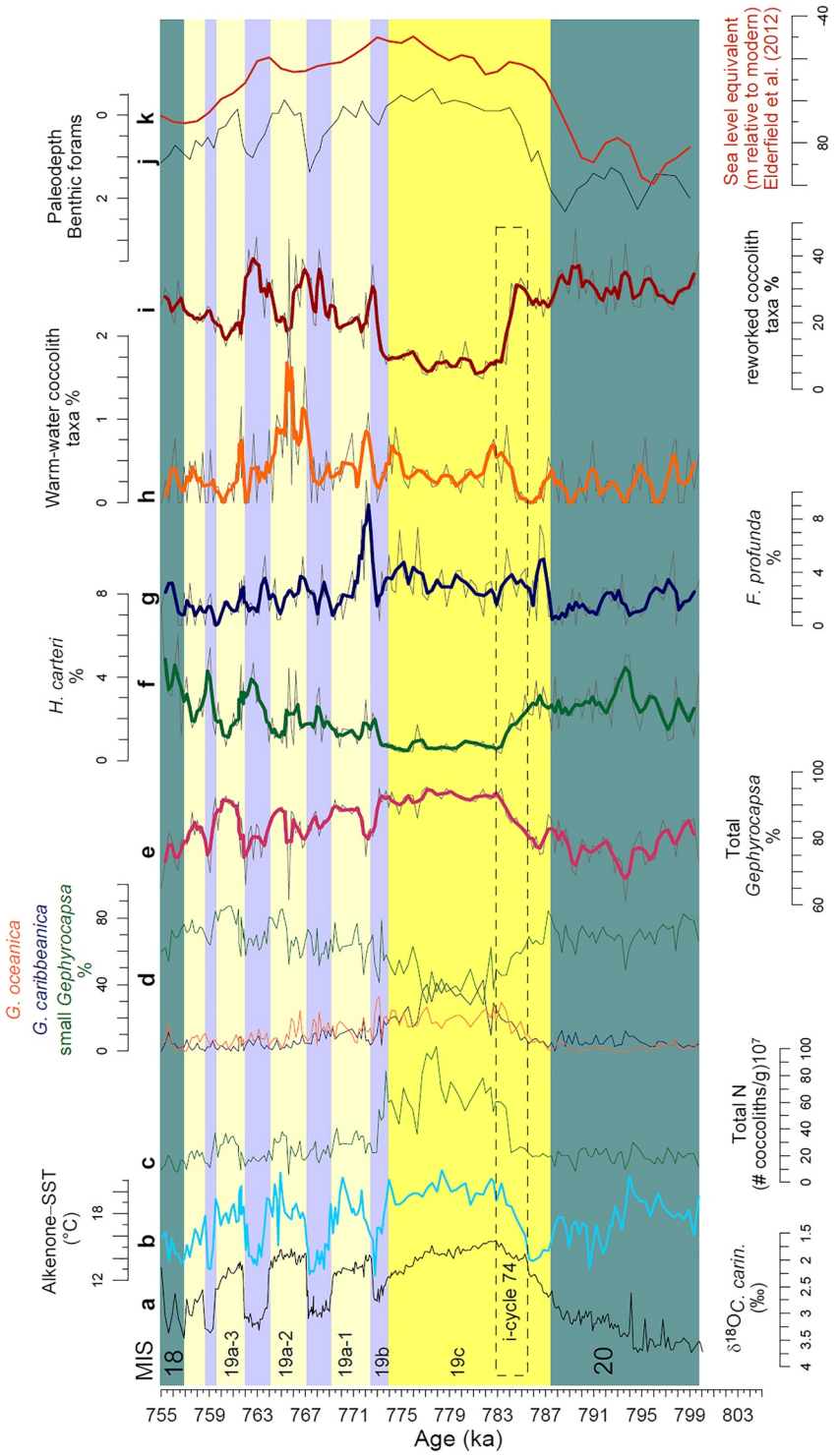

Figure 2. Benthic oxygen isotope (a) from Nomade et al. (2019) and alkenone-sea surface temperature (SST) records (b) from Marino et al. (2020) are compared with absolute (c) and relative (d)–(h) coccolithophore abundance at the Ideale section. Reworked coccolith taxa (i) are also shown and compared with paleodepth profile (j) at Ideale section (IS) (Stefanelli, 2003) and global sea level reconstruction plotted as sea level equivalent (m relative to modern) (k) from Elderfield et al. (2012). Dashed rectangle marks the sapropelic layer i-cycle 74 according to Maiorano et al. (2016) and Nomade et al. (2019).

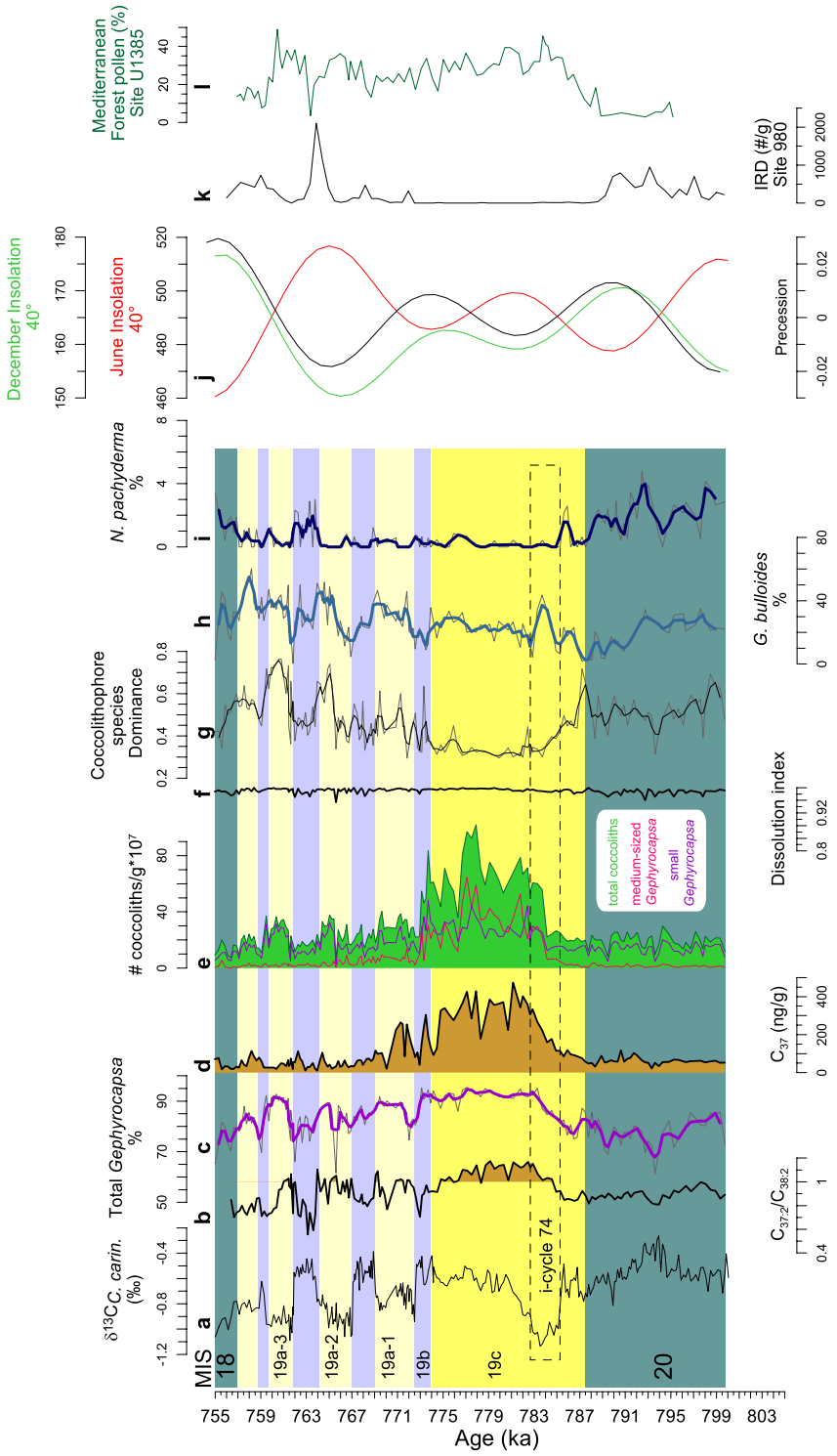

Figure 3. Carbon isotope record (a) from Nomade et al. (2019) compared with alkenone $C_{37:2}/C_{38:2}$ (b) and C_{37} patterns (d), coccolithophore relative (c) and absolute (e) abundances, dissolution index (f) and species dominance (g). *Globigerina bulloides* and polar-subpolar *Neogloboquadrina pachyderma* patterns at the Ideale section (h)–(i) are from Marino et al. (2020). Precession and insolation curves (j) are according to Laskar et al. (2004). Ice rafted debris (IRD) at ODP Site 980 (k) is from Wright and Flower (2002); Mediterranean forest pollen taxa record at IODP Site U1385 (l) is from Sánchez Gõni et al. (2016). Colored bands trace glacial-interglacial and stadial-interstadial phases across late Marine Isotope Stage (MIS) 20 and early MIS 18 according to Nomade et al. (2019). Dashed rectangle marks the sapropelic layer i-cycle 74 according to Maiorano et al. (2016) and Nomade et al. (2019).

5. Discussion

5.1. Paleoproductivity Proxies: Potential Interferences From Preservation/Dilution

Coccolith absolute abundance in the sediments may provide information on coccolithophore productivity in surface waters, although the effect of dissolution in water and/or at the sediment/water interface should be also considered (Flores et al., 2012). In the hemipelagic setting of the IS, variations in terrigenous input must also be considered. Similarly, changes in the concentrations of organic compounds can be controlled by preservation and/or terrigenous sediment dilution. The data set compiled here allows us to assess whether these complications override paleoproductivity signals, because they contain independent information of concentrations. As mentioned above, dissolution can be considered as negligible in the study section. In addition, changes in alkenone abundances (total C_{37}) mirror variations in the concentration of total coccoliths (Figures 3d and 3e), and, more specifically, of gephyrocapsids, likely the main producer of alkenones, suggesting that alkenone abundance mainly records past changes in alkenone accumulation rather than changes in the preservation of these biomarkers over time. In the modern ocean, alkenones are synthesized by a small group of haptophyte algae, restricted to the Noelaerhabdaceae family and specifically to *Emiliania huxleyi* and *G. oceanica* (Marlowe et al., 1990; Volkman et al., 1980, 1995), while in the Cenozoic record the topic on alkenone precursors is still debated (e.g., Athanasiou et al., 2017; Beltran et al., 2011; Plancq et al., 2012; Sicre et al., 2000; Villanueva et al., 2002). In the IS, *E. huxleyi* is absent due to the later appearance of the taxon, which occurs in the upper part of the Middle Pleistocene and thus the total N is mostly composed of gephyrocapsids that are mainly represented by small gephyrocapsids (small *G. caribbeanica* and small *Gephyrocapsa* with open central area) during MIS 20 and 19b-a (Figures 4a and 4d), and by medium-size *Gephyrocapsa* (*G. caribbeanica* and *G. oceanica* > 3 μm) during MIS 19c (Figures 4b and 4c). Despite the subject it is out of the main aim of the present study and conscious of the possible factors such as degradation, ecological conditions and alkenone contribution from non-calcifying species possibly involved in the relation between alkenone concentration and abundance of taxa (Beltran et al., 2011; Malinverno et al., 2008; Plancq, 2015; Prahl et al., 1989), we point out that the pattern of absolute abundance of *G. oceanica* and of *G. caribbeanica* displays similarities with that of total alkenone concentration, supported by positive correlations ($r = +0.80$ and $+0.82$, respectively; Figures 5c and 5d). This may imply, although not necessarily demonstrate, that these taxa are both the main alkenone producers during the studied interval, in agreement with recent data from the southern Indian Ocean during MIS 8 (Tangunan et al., 2021).

The good visual correspondence between alkenone concentration and total coccoliths through the record, although less evident at lower values, is associated with a high Pearson correlation coefficient ($r = +0.82$; Figure 5a). This is in agreement with previous observations made during the Holocene (Schwab et al., 2012; Weaver et al., 1999) and in the Pleistocene (Maiorano et al., 2015; Palumbo et al., 2013). The good correlation between the two proxies suggests that they can be used to reflect paleoproductivity variations in the IS.

A closer look at C_{37} and Total N shows that during MIS 20, and from MIS 19b upwards, C_{37} has rather low concentration with respect to the Total N (Figures 3d and 3e). It is noteworthy that alkenone concentration, although highly resistant, could be affected by degradation in the water column and in the sediment (Cacho et al., 2000; Grimalt et al., 2000; Madureira et al., 1995; Prahl et al., 1989, 1993, 2001; Sachs et al., 2000). A certain degree of degradation of C_{37} into the sediment has been observed during early diagenesis, depending on different oxygen content (Gong & Hollander, 1999; Rontani & Volkman, 2005). We cannot exclude the possibility that the lower concentration of C_{37} during MIS 20 and 19a may be related to enhanced degradation at the sea bottom, due to improved mixing/ventilation, as testified by the concomitant higher and/or strongly fluctuating $\delta^{13}C$ values (Nomade et al., 2019) (Figure 3a). However, studies on alkenone degradation do not find evidence of selective preservation of C_{37} relative to C_{38} alkenones (Prahl et al., 1989; Sinninghe Damsté et al., 2002).

Finally, considering the near-shore depositional setting of the IS, a dilution scenario for C_{37} alkenones and total coccolith abundance should be also discussed. In the IS, intervals of enhanced erosional processes and terrigenous input have been recorded during colder phases and low sea level (Maiorano et al., 2016). In this regard, we also examined changes in the relative proportions of $C_{37:2}/C_{38:2}$ as a potential paleoproductivity proxy. The $C_{37:2}/C_{38:2}$ ratio does not depend on the preservation or dilution controls that might affect total C_{37} alkenone concentrations. The $C_{37:2}/C_{38:2}$ ratio is chosen because both are diunsaturated methyl ketones

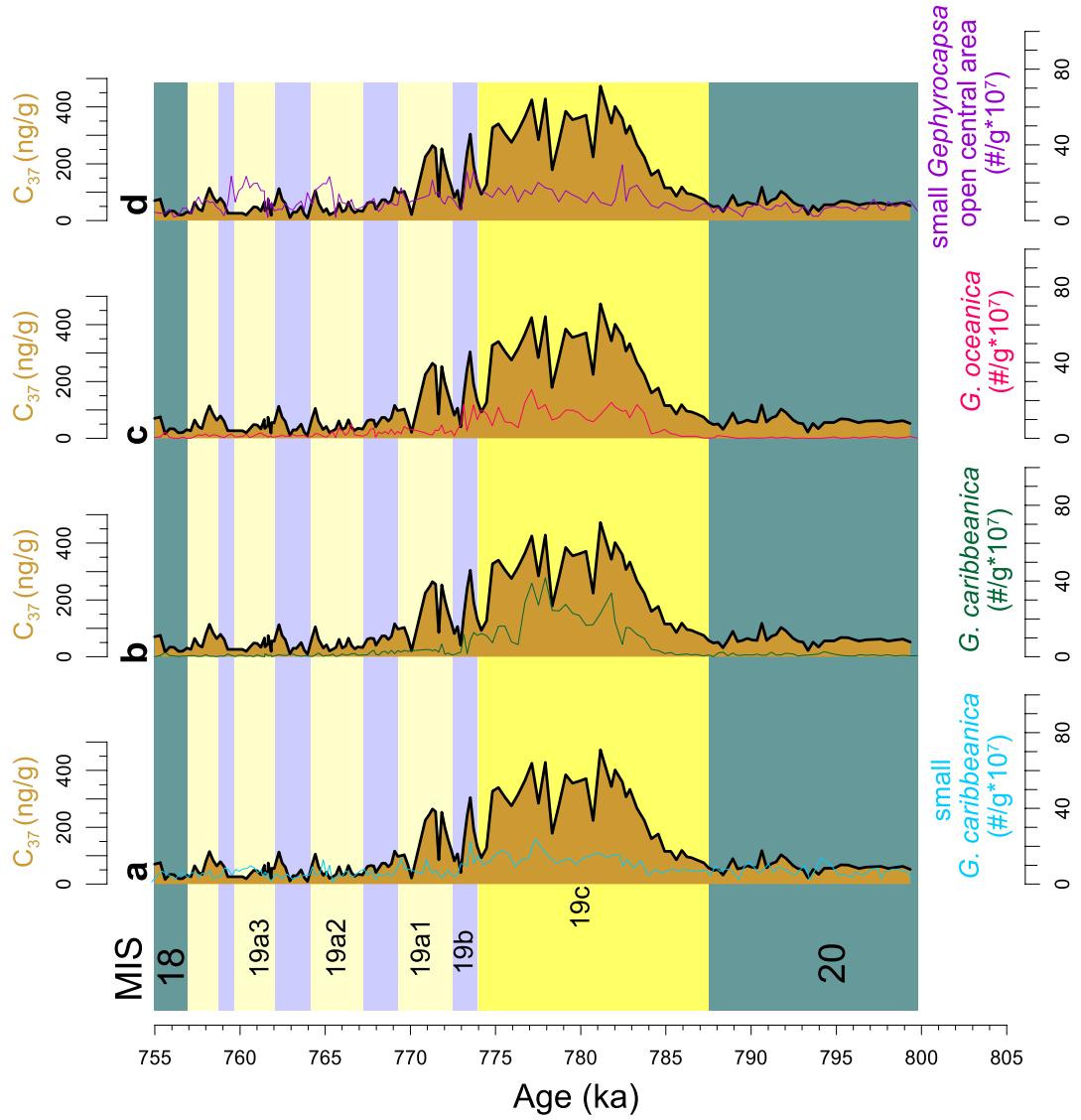

Figure 4. Gephyrocapsid absolute abundances (#/g) plotted against C_{37} concentration at the Ideale section. Colored bands trace glacial-interglacial and stadial-interstadial phases across late Marine Isotope Stage (MIS) 20 and early MIS 18 according to Nomade et al. (2019).

(there is also a $C_{38:3}$ ethyl ketone measured). Because these are homologous (methyl ketone) compounds, they should have similar temperature dependence as shown by the tight covariance of the U^k_{37} and U^k_{38} (methyl) unsaturation indices (Herbert, 2014; Figure 2). Therefore any variation in the $C_{37:2}/C_{38:2}$ ratio does not arise from a temperature control, but instead from a physiologically driven change in allocation of chain length during alkenone synthesis. Paleoecological factors involved in changing the ratio are not clear and could arise from changes in the alkenone producers over time, or from physiological reasons for changing contribution in C_{37} to C_{38} alkenone synthesis in response to environmental factors. The index seems to correspond to well-known oligotrophic-eutrophic cycles in the Plio-Pleistocene of the Eastern Mediterranean (Herbert et al., 2015). The IS record displays a positive, although moderate correlation ($r = +0.59$) between $C_{37:2}/C_{38:2}$ ratio and the total number of coccoliths as well (Figure 5b) suggesting that, although a dilution effect likely occurred in the study section, the primary signal was conserved. This alkenone ratio and its comparison with total coccolith abundance is the first of its kind documented so far in the literature. Its positive correlation with changes in total coccolith abundance (mainly with placolith-bearing taxa) may indicate a relation with paleoecological conditions and encourage future investigations on the usefulness

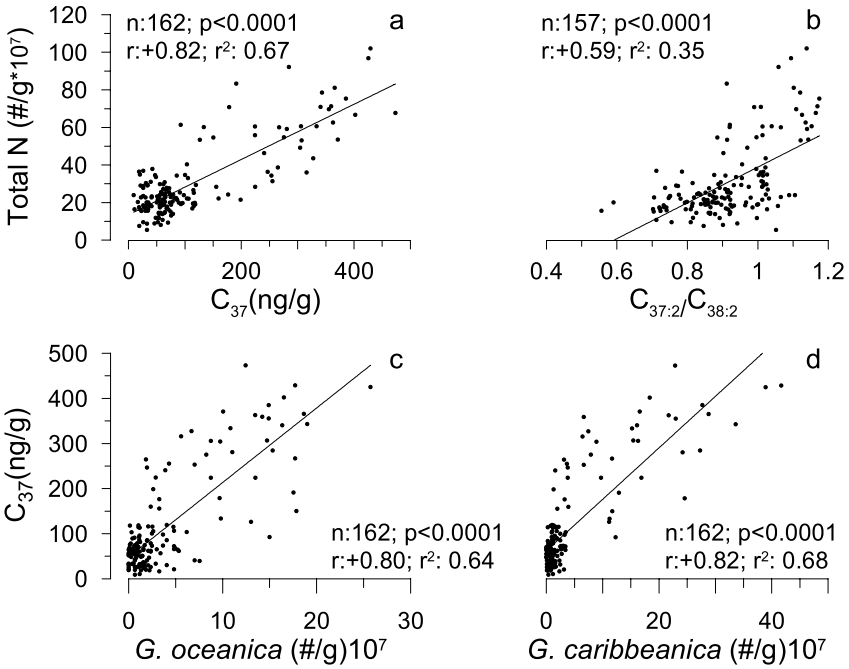

Figure 5. Scattered plot of total coccolithophore abundance (Total N) versus C_{37} (a) and $C_{37:2}/C_{38:2}$ (b) and of gephyrocapsid absolute abundances versus C_{37} (c)–(d) based on Pearson correlation results.

of this proxy. Taking into account potential interferences, the independent micropaleontological (Total N) and organic (C_{37} and $C_{37:2}/C_{38:2}$) paleoproductivity proxies, through the IS, highlight low productivity values during MIS 20 (Figures 3b, 3d and 3e), increased productivity during most of MIS 19c and fluctuating values during MIS 19a, following interstadial-stadial oscillations, the latter primarily marked by the pattern of Total N and $C_{37:2}/C_{38:2}$ ratio.

5.2. Main Shifts in the Coccolithophore Community: Productivity Versus Turbidity

We compared the paleoproductivity proxies with the relative abundance of the most important component of the coccolithophore assemblage, that is, the placoliths-bearing taxa belonging to the genus *Gephyrocapsa* (Figure 3c). Placoliths are r-strategist taxa that bloom after nutrient fertilization and their abundance variation is considered a proxy of high productivity conditions (Broerse et al., 2000; Flores et al., 2000; López-Otálvaro et al., 2008; Young, 1994). They are characteristic of meso to eutrophic environments, such as upwelling areas and shelf seas (Baumann et al., 2005). In order to avoid here again potential dilution effect, we solely relied on the relative abundance of specific taxa that provides biological information independently from sedimentological effect (Gibbs et al., 2012). The oscillating distribution pattern of the total gephyrocapsids (Figure 3c) indicates that the parameters controlling their proliferation frequently switched through time, with persistent low/high productivity occurring during MIS 20/MIS 19c, and a fluctuating pattern from MIS 19b upwards, with enhanced productivity during warmer and wetter interstadials. The total gephyrocapsid distribution through time (Figure 3c) parallels fluctuations of the $C_{37:2}/C_{38:2}$ ratio (Figure 3b). From a paleoecological point of view, placolith relative increases alternate with those of *H. carteri* (Figure 2f), as shown by their strong inverse correlation ($r = -0.82$; Figure S2). *H. carteri* benefits from turbid upper water layer (Bonomo et al., 2014, 2021; Colmenero-Hidalgo et al., 2004; Maiorano et al., 2019) and is a species with neritic affinity (Aizawa et al., 2004; Dimiza et al., 2014; Okada, 1992). Thus, decreased placolith abundances versus increase of *H. carteri* during cold phases may reflect enhanced turbidity and decrease in the light intensity in surface water. The positive, although moderate correlation of *H. carteri* with reworked coccoliths ($r = +0.55$; Figure S2), a valuable proxy of higher continental input (Bonomo et al., 2016; Colmenero-Hidalgo et al., 2004; Flores et al., 1997; Maiorano et al., 2016) supports the relation of the taxon with turbid surface water. In the Montalbano Jonico section, more specifically, the abundance of reworked coccoliths is related with the pattern of local paleodepth changes (Figure 2j) and global

sea level reconstruction (Figure 2k), with increasing values during low sea level phases (i.e., during drier glacial/stadial phases) when more efficient erosion on land prevailed (Maiorano et al., 2016). The results indicate that increased land-derived nutrient from river input, during warm and wetter conditions, and enhanced turbidity consequent of improved continental erosion during colder and drier climate were important forcing mechanism modulating coccolithophore productivity in the near-shore depositional setting of the IS. However, within the placolith-bearing taxa, prominent shifts between small and medium-sized taxa did occur over time (Figure 2d) and were likely forced by climate-induced paleoenvironmental variations.

5.3. Glacial-Interglacial Productivity Mode

Productivity in the IS mainly shifts between a cold-low productivity to warm-high productivity scenario, with a distinct change in terms of assemblage variations occurring between glacial MIS 20 and full interglacial MIS 19c. During MIS 20, small *Gephyrocapsa* largely dominate among the placoliths (Figure 2d), representing the most important group within the total coccolith abundance (Figure 3e). It is well known that small *Gephyrocapsa*, which inhabit the upper photic zone, are opportunistic taxa showing a rapid response to nutrients availability and provide a proxy of high productivity and unstable surface waters (Gartner, 1988; Hernández-Almeida et al., 2011; Knappertsbusch, 1993; Marino et al., 2011, 2018; Takahashi & Okada, 2000). Therefore, the dominance of small *Gephyrocapsa* at the IS during MIS 20 (Figure 2d) suggests high-nutrient availability and water-mixing in surface water; low relative abundances of the deep dwelling taxon *F. profunda* (Figure 2g) in the same interval, support nutrient availability in surface water, shallow nutricline and reduced seasonal stratification as the dominant controls on productivity (Beaufort et al., 1997, 2001; McIntyre & Molfino, 1996; Molfino and McIntyre, 1990a, 1990b). The occurrence of *G. bulloides* (Figure 3h) is consistent with nutrient availability in surface water related to wind-induced vertical mixing during cold and arid climate, while the presence of *N. pachyderma* (Figure 3i) suggests polar-subpolar water incursion into the Mediterranean (Cacho et al., 1999; Capotondi et al., 2016; Girone et al., 2013; Marino et al., 2018; Pérez-Folgado et al., 2003; Sierro et al., 2005) and at the site location. Both marine and continental proxies support colder-drier conditions during MIS 20 in the IS (Figure 1C; Bertini et al., 2015; Maiorano et al., 2016; Marino et al., 2020; Nomade et al., 2019), which are likely related to enhanced north-westerly winds, adequate mixing and nutrient availability in surface water. Despite the flourishing of the highly productive small *Gephyrocapsa* group (Figure 2d), Total N, C_{37} and $C_{37:2}/C_{38:2}$ indicate that coccolithophore productivity in surface waters remains rather low during this phase (Figures 3b, 3d and 3e), with respect to other periods. Less negative $\delta^{13}C$ values during this part of the record also support reduced carbon supply and enhanced ventilation at the seafloor (Figure 3a). It is reasonable to hypothesize that colder glacial conditions and polar water influx (increase of *N. pachyderma*—Figure 3i), likely combined with surface water turbidity (increased abundance of *H. carteri*—Figure 2f) created unfavorable environmental conditions that prevented the proliferation of the coccolithophores during late MIS 20 as indicated by low values of total coccolithophore abundance.

On the other hand, Total N, C_{37} and $C_{37:2}/C_{38:2}$ ratio reach maximum values during most of MIS 19c (Figures 3b, 3d and 3e), that is, the climatically stable part of interglacial MIS 19 in the IS (Nomade et al., 2019), indicating a marked increase of coccolithophore productivity. In fact, total gephyrocapsids reach their highest relative and absolute abundances during this phase as well (Figures 3c and 3e). The most significant shift in the assemblage is marked by the recovery of medium-sized *Gephyrocapsa* and a strong reduction in the species dominance (Figure 3g) suggesting a well-diversified coccolithophore community. Within the medium-sized group, *G. oceanica* is a common component of low-latitude assemblages (Baumann et al., 2005; Boeckel & Baumann, 2004; Haidar & Thierstein, 2001; Winter et al., 1994; Ziveri et al., 2004) and related to less saline Atlantic inflow in the Mediterranean Sea (Álvarez et al., 2010; Bárcena et al., 2004; Bazzicalupo et al., 2018, 2020; Knappertsbusch, 1993; Oviedo et al., 2017) especially during sea level highstand. On the other hand, *G. caribbeanica* is considered a cosmopolitan taxon (Baumann & Freitag, 2004; Flores et al., 2012; Saavedra-Pellitero et al., 2017) with a more questionable ecology since it has been related to oligotrophic and warm surface waters (Bollmann, 1997; Bollmann et al., 1998; Toti et al., 2020), to seasonally nutrient-enriched subpolar to subtropical waters (Baumann & Freitag, 2004). This species is capable of seasonal bloom (Baumann et al., 2005; Flores et al., 2012), and usually used as a proxy for high paleoproductivity (González-Lanchas et al., 2020; López-Otálvaro et al., 2008; Maiorano et al., 2013; Quivelli et al., 2020). The increase of medium-sized *Gephyrocapsa* and their significant contribution to

coccolithophore abundance during MIS 19c, with respect to MIS 20 can be interpreted as a marked change in the paleoenvironment and specifically associated with a persistent warmer environment (SSTs are persistently at their maxima values, with mean values of about 18.5°C; Figure 2b) as well as adequate, seasonal nutrient availability that sustained placolith spring/winter blooming. Nutrients were likely replenished from continental supply through precipitations and vertical mixing during winter.

The persistent occurrence of *G. bulloides* (Figure 3h) supports seasonal sea surface water nutrient availability, likely related to river run-off during the winter-spring period, that is, when *G. bulloides* proliferates. It is noteworthy that thanks to the high-sedimentation rate and the sampling resolution it is possible to observe that the onset of the enhanced coccolithophore productivity during MIS 19c does not develop earlier than the upper portion of the sapropelic layer related to i-cycle 74 (Figure 3), as testified by the gradual increase of Total N, C_{37} and $C_{37:2}/C_{38:2}$. This is likely in relation with enhanced turbidity associated with the increase in precipitation/river runoff accompanying the lowermost sapropel portion during insolation maximum (Marino et al., 2020). This hypothesis is supported by the prominent peak of reworking (Figure 2i) and also of *G. bulloides* (Figure 3h) that, thanks to its opportunistic behavior, likely exploited enhanced nutrient from land during increased river input. The scenario during MIS 19c is in agreement with the climate framework reconstructed at the IS during this time period, which is characterized by climate improvement on land as suggested by the main expansion of temperate forest, dominated by broad-leaved trees typical of a (warm) temperate and relatively humid climate, with mild winters and warm summers and a seasonal precipitation regime (Bertini et al., 2015; Maiorano et al., 2016; Nomade et al., 2019). The latter provided adequate seasonal external input of nutrients from river runoff which, together with warmer surface water conditions, ensured the highest coccolithophore productivity.

5.4. Stadial/Interstadial Productivity Variations

From MIS 19b onwards, alternating warm-cold paleoproductivity scenario is observed on a short-term time scale as well, matching stadial-interstadial variations. It has been documented that in this part of the section marked millennial-scale drying and cooling events alternate with wetter and warmer phases, as proved by distinct shifts in the Mesothermic arboreal pollen taxa (Figure 1C) coupled with sharp SST and oxygen and carbon isotope changes (Maiorano et al., 2016; Marino et al., 2020; Nomade et al., 2019). They reflect not only local environmental changes but also short-term climate instability recorded on a global scale, during the transition toward the MIS 18 glacial inception in North Atlantic (Emanuele et al., 2015; Ferretti et al., 2015; Kleiven et al., 2011), at the Iberian margin (Sánchez Gõni et al., 2016) and in the Mediterranean region, in both marine (Marino et al., 2015, 2016; Nomade et al., 2019; Toti et al., 2020) and continental records (Giaccio et al., 2015; Mangili et al., 2007; Regattieri et al., 2019). The millennial-scale productivity changes we observe during MIS 19a points toward enhanced productivity during interstadials relative to stadials. This pattern is less evident in the C_{37} profile, likely due to the low concentration of total alkenones and the potential effects of preservation and/or dilution of biomarkers as discussed above. A rapid shift in the coccolithophore community occurred as shown by the increase of small *Gephyrocapsa* and of species dominance (Figure 3g), indicating a rather unstable, nutrient-rich surface water environment developed during interstadials. Indeed, the contribution of medium-sized *Gephyrocapsa* to Total N during MIS 19a warm oscillations is negligible, if compared with MIS 19c warm scenario, as shown by their rather low absolute abundances (Figure 3e). Despite the relevant shift in terms of gephyrocapsid assemblage, surface water temperature did not change significantly between MIS 19c and MIS 19a interstadials (Figure 2b), thus suggesting that temperature was not the primary parameter hampering or reducing the proliferation of medium-sized *Gephyrocapsa* in the assemblage during warm episodes of MIS 19a. Within the foraminiferal assemblage, the long-term increasing trend of *G. bulloides* during MIS 19a, and at shorter scale during interstadials (Figure 3h), supports enhanced nutrient availability in surface water. It is noteworthy that MIS 19a occurs when precession index is at minimum (Figure 3i), an orbital configuration leading to northward penetration of the ITCZ promoting intensified summer aridity and enhanced winter precipitation in the region (e.g., Milner et al., 2012; Nomade et al., 2019; Regattieri et al., 2015; Tzedakis, 2007; Wagner et al., 2019). It is therefore likely that enhanced productivity during interstadials was primarily promoted by the increased land-derived nutrient availability through river discharges from neighboring land, during more pronounced wetter winters, rapidly exploited by r-strategist small *Gephyrocapsa* group. In this scenario, an increased influence of the WAC may have also contributed to the nutrient delivery in the study area.

A contribution from local upwelling resulting from improved advection of Atlantic water during sea level rise that goes along with interstadials (Figure 1C), as occurs today at the periphery of the anticyclonic NIG (Batistić et al., 2014, 2017; Civitarese et al., 2010), cannot be also excluded.

Looking in more detail at the evolution of MIS 19 interstadials, their earlier portions are generally marked by a slight increase in the abundance of *F. profunda* (Figure 2g), suggesting deeper nutricline and lower productivity in surface water (e.g., Beaufort et al., 1997; Molfino & McIntyre, 1990a, 1990b). It is likely that the abrupt shift in SST accompanying the onset of each interstadial (Figure 2b) promoted strong summer thermocline favoring *F. profunda* and low nutrient contents at sea surface waters, as indicated by low abundances of *G. bulloides* (Figure 3h). Then, a shallowing in the nutricline depth, from a distinct Deep Chlorophyll Maximum (DCM) to highly productive surface water is observed in the course of each interstadial (slight decrease of *F. profunda*, increase of Total N, small *Gephyrocapsa* and *G. bulloides*), likely reflecting the land-derived nutrient enrichment in surface water and possible local upwelling. A similar pattern in the interstadial evolution has been also observed in the Sicily Channel (Incarbona et al., 2013). On the other hand, during stadial phases, the pronounced SST decrease (Figure 2b), reaching minima of 12–13°C at the IS, coupled with enhanced surface water turbidity (marked increase of *H. carteri* and reworking) occurring during drier phases, were likely unfavorable conditions even for small gephyrocapsids and may explain the reduction in total coccolithophore productivity.

Exacerbated summer aridity likely developed during MIS 19a-2, at the precession minimum peak (Figure 3j). Differently from the other interstadials, MIS 19a-2 records a marked increase of WWCT (Figure 2h). The more oligotrophic conditions in surface waters developed during maximum summer aridity on land (reduced nutrient supply from land), favoring the vertical taxon zonation in the Mediterranean (Knappertsbusch, 1993; Oviedo et al., 2015) and the increase of WWCT that benefit from warm and oligotrophic waters (Baumann et al., 2004; Boeckel & Baumann, 2004; McIntyre & Bé, 1967; Palumbo et al., 2013; Saavedra-Pellitero et al., 2010; Winter et al., 1994; Ziveri et al., 1995, 2004). It is worth noticing the stadial part of MIS 19a-2, that is characterized by the distinct increase of *N. pachyderma* with respect to the other stadials (Figure 3i). The incursion of the polar taxon clearly marks enhanced arrival of cold polar water in the Mediterranean and in the Ionian basin, likely related to ice-sheet instability in the North Atlantic. This hypothesis is strengthened by the increase of *N. pachyderma* in the western Mediterranean at ODP Site 975 (Quivelli, 2020) during the same stadial phase. Finally, this cold water arrival is probably linked to the Ice Rafted Debris (IRD) peak recorded at ODP Site 980 in North Atlantic (Wright & Flower, 2002), as well as enhanced freshwater pulse at the Iberian Margin (Rodrigues et al., 2017). This phase is also marked by a peak of Mediterranean forest pollen taxa decrease (Sánchez Gõni et al., 2016; Figure 3l), suggesting aridity on land and the worldwide relevance of this iceberg discharge event. At the IS the sharp coeval depletion observed in the $C_{37:2}/C_{38:2}$ ratio (Figure 3b) may reflect a relevant impact of this event on coccolithophore productivity in relation with enhanced arrival of cold and low salinity surface water, hampering biological productivity as observed during the last glacial stadial phases (Colmenero-Hidalgo et al., 2004; Incarbona et al., 2013).

The observed warm-cold millennial-scale productivity mode in the IS during MIS 19a appears rather comparable to the pattern observed in the Alboran Sea (Cacho et al., 2000; Colmenero-Hidalgo et al., 2004; Moreno et al., 2005) and in the Sicily Channel (Incarbona et al., 2013) during Dansgaard-Oeschger oscillations of the last 70 kyr, indicating a similar productivity dynamic in different areas, depositional settings and time intervals. It is noteworthy that both in the Alboran Sea and in the Sicily Channel the stadial/low productivity and interstadial/high productivity pattern in the last glacial period is marked by relative increase of small placoliths during Interstadials and of *H. carteri* and *Syracosphaera* spp. during Stadials and Heinrich events (Colmenero-Hidalgo et al., 2004), similarly to the result in the IS. The strong relation between placoliths and *H. carteri* at the IS, the documented vegetation changes, consistent with the climate framework in southern Europe at Site U1385 (Sánchez Gõni et al., 2016), in central (Regattieri et al., 2019) and northern Italy (Moscariello et al., 2000; Rossi, 2003), as discussed by Nomade et al. (2019), suggests that the productivity pattern in the IS was the local response to the basin-wide warmer and wetter conditions during MIS 19 interstadials, resulting from the southward positions of the westerlies, which provided enhanced humidity over the Mediterranean region. This pattern would have promoted a shift from low basinal nutrient inventory during cold and arid phases to a higher nutrient budget in warm and humid

periods. This productivity scenario appears also in line with the modern seasonal variability observed in the coccolithophore export production in the eastern Mediterranean, which documents enhanced productivity during the late winter-spring season, associated with water column mixing and increased rainfall rate (Malinverno et al., 2009; Triantaphyllou et al., 2010).

6. Conclusion

We obtained a high temporal resolution data set of coccolithophores and organic biomarkers, which provides evidence of climate-induced productivity variations in the central Mediterranean at millennial-scale in a near-shore environment. The patterns of Total N, alkenone parameters, that is, C_{37} and $C_{37:2}/C_{38:2}$ ratio, compared with the relative abundance of coccolithophore blooming species (gephyrocapsids), *H. carteri*, reworked coccolith taxa and few planktonic foraminifera species, make it possible to propose a paleoproductivity scenario from late MIS 20 to earliest MIS 18. Our main results include not only the first Mediterranean documentation of C_{37} total concentration during the late MIS 20-early MIS 18, but also the use of $C_{37:2}/C_{38:2}$ ratio as a paleoenvironmental proxy. The pattern of this ratio mirrors the profiles of those taxa related to productivity, thus encouraging future investigations in different depositional settings. Potential interferences from dilution and degradation phenomena have been taken into account and cannot fully be excluded in the study section. However, a primary ecological signal is recognizable in our record since the integrated data set shows consistent patterns, which sustain their use as paleoproductivity signals in a near-shore environment. The resulting cold/low- to warm/high- productivity scenario matches glacial-interglacial and stadial-interstadial variations. Low productive surface water resulted from enhanced surface water turbidity developing during prevalent erosion process on land and low sea level and from cold-water conditions and polar-subpolar low salinity water incursion into the Mediterranean. The higher coccolithophore productivity during warm MIS 19c was sustained by persistent warmer surface waters coupled with a seasonal precipitation regime and consequent nutrient availability. Millennial-scale low-high productivity variations mirror stadial-interstadial phases. Enhanced productivity during interstadials was likely promoted by the increased land-derived nutrients through river discharge during more pronounced wetter winters. Specifically, increased SST firstly developed a summer thermocline and oligotrophic surface water conditions at the onset of each interstadial, while enhanced nutrient supply from land and local upwelling promoted a shallow nutricline and highly productive surface water during the late interstadials. This short-term scenario is rather very similar to evidences brought from deep-sea records from central and western Mediterranean during Dansgaard-Oeschger oscillations of the last 70 kyr, highlighting a comparable productivity dynamic in different time intervals and depositional settings. Our results suggest a common regional forcing over time that mirrors the changing westerlies position and related humidity over the Mediterranean region and the periodic North Atlantic water inflow of polar origin. Finally, comparison of alkenone patterns with that of the coccolithophore assemblages suggests the gephyrocapsid group, essentially the medium-size morphotypes, as the main alkenone contributor in the studied interval.

Data Availability Statement

In the present version, data are available via supplements. The new data supporting figures of the present manuscript are deposited on https://data.mendeley.com/datasets/38rvfnvmt3/1.

Acknowledgments
This research study was financially supported by Università degli Studi di Bari Aldo Moro, Fondi di Ateneo P. Maiorano, 2018 and benefited of instrumental upgrades from "Potenziamento Strutturale PONa3_00369 dell'Università degli Studi di Bari, Laboratorio per lo Sviluppo Integrato delle Scienze e delle TEcnologie dei Materiali Avanzati e per dispositivi innovativi (SISTEMA)." T. D. Herbert acknowledges financial support from National Science Foundation OCE-1459280. The authors thank the editor and two anonymous referees, who improved the first version of the manuscript.

References

Aiello, G., Barra, D., & Parisi, R. (2015). Lower-Middle Pleistocene ostracod assemblages from the Montalbano Jonico section (Basilicata, southern Italy). *Quaternary International*, *383*, 47–73. https://doi.org/10.1016/j.quaint.2014.11.010

Aizawa, C., Oba, T., & Okada, H. (2004). Late Quaternary paleoceanography deduced from coccolith assemblages in a piston core recovered of the central Japan coast. *Marine Micropaleontology*, *52*, 277–297. https://doi.org/10.1016/j.marmicro.2004.05.005

Álvarez, M. C., Amore, O. F., Cros, L. L., Alonso, B., Alcántara-Carrió, J., De España, M., et al. (2010). Coccolithophore biogeography in the Mediterranean Iberian margin. *Revista Espanola de Micropaleontologia*, *42*, 359–371.

Amore, F. O., Flores, J. A., Voelker, A. H. L., Lebreiro, S. M., Palumbo, E., & Sierro, F. J. (2012). A Middle Pleistocene Northeast Atlantic coccolithophore record: Paleoclimatology and paleoproductivity aspects. *Marine Micropaleontology*, *90–91*, 44–59. https://doi.org/10.1016/j.marmicro.2012.03.006

Artegiani, A., Paschini, E., Russo, A., Bregant, D., Raicich, F., & Pinardi, N. (1997). The Adriatic Sea general circulation. Part I: Atmospheric sea interactions and water mass structure. *Journal of Physical Oceanography*, *27*(8), 1492–1514. https://doi.org/10.1175/1520-0485(1997)027<1492:TASGCP>2.0.CO;2

Athanasiou, M., Bouloubassi, I., Gogou, A., Klein, V., Dimiza, M. D., Parinos, C., et al. (2017). Sea surface temperatures and environmental conditions during the "warm Pliocene" interval (~4.1–3.2 Ma) in the Eastern Mediterranean (Cyprus). *Global and Planetary Change*, *150*, 46–57. https://doi.org/10.1016/j.gloplacha.2017.01.008

Ausín, B., Flores, J. A., Sierro, F. J., Bárcena, M. A., Hernández-Almeida, I., Frances, G., et al. (2015). Coccolithophore productivity and surface water dynamics in the Alboran Sea during the last 25 kyr. *Palaeogeography, Palaeoclimatology, Palaeoecology*, *418*, 126–140. https://doi.org/10.1016/j.palaeo.2014.11.011

Ausín, B., Flores, J. A., Sierro, F. J., Cacho, I., Hernández-Almeida, I., Martrat, B., & Grimalt, J. O. (2015). Atmospheric patterns driving Holocene productivity in the Alboran Sea (Western Mediterranean): A multiproxy approach. *The Holocene*, *25*(4), 583–595. https://doi.org/10.1177/0959683614565952

Bárcena, M. A., Flores, J. A., Sierro, F. J., Pérez-Folgado, M., Fabres, J., Calafat, A., & Canals, M. (2004). Planktonic response to main oceanographic changes in the Alboran Sea (Western Mediterranean) as documented in sediment traps and surface sediments. *Marine Micropaleontology*, *53*(3–4), 423–445. https://doi.org/10.1016/j.marmicro.2004.09.009

Batistić, M., Garić, R., & Molinero, J. C. (2014). Interannual variations in Adriatic ´ Sea zooplankton mirror shifts in circulation regimes in the Ionian Sea. *Climate Research*, *61*, 231–240. https://doi.org/10.3354/cr0124810.3354/cr01248

Batistić, M., Viličić, D., Kovačević, V., Jasprica, N., Lavignec, H., Carića, M., et al. (2017). Winter phytoplankton blooms in the offshore south Adriatic waters (1995-2012) regulated by hydroclimatic events: Special emphasis on the exceptional bloom of 1995. *Biogeosciences Discussions*. https://doi.org/10.5194/bg-2017-205

Baumann, K.-H., Andruleit, H., Böckel, B., Geisen, M., & Kinkel, H. (2005). The significance of extant coccolithophores as indicators of ocean water masses, surface water temperature, and paleoproductivity: A review. *Paläontologische Zeitschrift*, *79*(1), 93–112. https://doi.org/10.1007/bf03021756

Baumann, K.-H., Bockel, B., & Frenz, M. (2004). Coccolith contribution to South Atlantic carbonate sedimentation. In H. R. Thierstein, & Y. R. Young (Eds.), *Coccolithophores* (pp. 367–402). Springer. https://doi.org/10.1007/978-3-662-06278-4_14

Baumann, K.-H., & Freitag, T. (2004). Pleistocene fluctuations in the northern Benguela Current system as revealed by coccolith assemblages. *Marine Micropaleontology*, *52*, 195–215. https://doi.org/10.1016/j.marmicro.2004.04.011

Bazzicalupo, P., Maiorano, P., Girone, A., Marino, M., Combourieu-Nebout, N., & Incarbona, A. (2018). High-frequency climate fluctuations over the last deglaciation in the Alboran Sea, Western Mediterranean: Evidence from calcareous plankton assemblages. *Palaeogeography, Palaeoclimatology, Palaeoecology*, *506*, 226–241. https://doi.org/10.1016/j.palaeo.2018.06.042

Bazzicalupo, P., Maiorano, P., Girone, A., Marino, M., Combourieu-Nebout, N., Pelosi, N., et al. (2020). Holocene climate variability of the Western Mediterranean: Surface water dynamics inferred from calcareous plankton assemblages. *The Holocene*, *30*(5), 691–708. https://doi.org/10.1177/0959683619895580

Beaufort, L., de Garidel-Thoron, T., Mix, A. C., & Pisias, N. G. (2001). ENSO-like forcing on oceanic primary production during the Late Pleistocene. *Science*, *293*, 2440–2444. https://doi.org/10.1126/science.293.5539.2440

Beaufort, L., Lancelot, Y., Camberlin, P., Cayre, O., Vincent, E., Bassinot, F., & Labeyrie, L. (1997). Indian Ocean primary production insolation cycles as a major control of Equatorial Indian Ocean primary production. *Science*, *278*(5342), 1451–1454. https://doi.org/10.1126/science.278.5342.1451

Beltran, C., Flores, J.-A., Sicre, M.-A., Baudin, F., Renard, M., & de Rafélis, M. (2011). Long chain alkenones in the Early Pliocene Sicilian sediments (Trubi Formation—Punta di Maiata section): Implications for the alkenone paleothermometry. *Palaeogeography, Palaeoclimatology, Palaeoecology*, *308*, 253–263. https://doi.org/10.1016/j.palaeo.2011.03.017

Bertini, A., Toti, F., Marino, M., & Ciaranfi, N. (2015). Vegetation and climate across the Early-Middle Pleistocene transition at the Montalbano Jonico section (southern Italy). *Quaternary International*, *383*, 74–88. https://doi.org/10.1016/j.quaint.2015.01.003

Béthoux, J. P., Morin, P., Chaumery, C., Connan, O., Gentili, B., & Ruiz-Pino, D. (1998). Nutrients in the Mediterranean Sea, mass balance and statistical analysis of concentrations with respect to environmental change. *Marine Chemistry*, *63*, 155–169. https://doi.org/10.1016/S0304-4203(98)00059-0

Bignami, F., Sciarra, R., Carniel, S., & Santolieri, R. (2007). Variability of Adriatic Sea coastal turbid waters from SeaWiFS imagery. *Journal of Geophysical Research*, *112*, C03S10. https://doi.org/10.1029/2006jc003518

Boeckel, B., & Baumann, K.-H. (2004). Distribution of coccoliths in surface sediments of the south-eastern South Atlantic Ocean: Ecology, preservation and carbonate contribution. *Marine Micropaleontology*, *51*(3–4), 301–320. https://doi.org/10.1016/j.marmicro.2004.01.001

Bollmann, J. (1997). Morphology and biogeography of *Gephyrocapsa* coccoliths in Holocene sediments. *Marine Micropaleontology*, *29*, 319–350. https://doi.org/10.1016/S0377-8398(96)00028-X

Bollmann, J., Baumann, K.-H., & Thierstein, H. R. (1998). Global dominance of *Gephyrocapsa* coccoliths in the late Pleistocene: Selective dissolution, evolution, or global environmental change? *Paleoceanography*, *13*(5), 517–529. https://doi.org/10.1029/98PA00610

Bonomo, S., Cascella, A., Alberico, I., Ferraro, L., Giordano, L., Lirer, F., et al. (2014). Coccolithophores from near the Volturno estuary (central Tyrrhenian Sea). *Marine Micropaleontology*, *111*, 26–37. https://doi.org/10.1016/j.marmicro.2014.06.001

Bonomo, S., Cascella, A., Alberico, I., Sorgato, S., Pelosi, N., Ferraro, L., et al. (2016). Reworked Coccoliths as runoff proxy for the last 400 years: The case of Gaeta gulf (central Tyrrhenian Sea, Central Italy). *Palaeogeography, Palaeoclimatology, Palaeoecology*, *459*, 15–28. https://doi.org/10.1016/j.palaeo.2016.06.037

Bonomo, S., Schroeder, K., Cascella, A., Alberico, I., & Lirer, F. (2021). Living coccolithophore communities in the central Mediterranean Sea (Summer 2016): Relations between ecology and oceanography. *Marine Micropaleontology*, *165*, 101995. https://doi.org/10.1016/j.marmicro.2021.101995

Brand, L. E. (1994). Physiological ecology of marine coccolithophores. In A. Winter, & W. G. Siesser (Eds.), *Coccolithophores* (pp. 39–49). Cambridge University Press.

Broerse, A. T. C., Ziveri, P., van Hinte, J. E., & Honjo, S. (2000). Coccolithophore export production, species composition, and coccolith-$CaCO_3$ fluxes in the NE Atlantic (34°N 21°W and 48°N 21°W). *Deep-Sea Research Part II: Topical Studies in Oceanography*, *47*, 1877–1905. https://doi.org/10.1016/S0967-0645(00)00010-2

Cacho, I., Grimalt, J. O., & Canals, M. (2002). Response of the Western Mediterranean Sea to rapid climatic variability during the last 50,000 years: A molecular biomarker approach. *Journal of Marine Systems*, *33*, 253–272. https://doi.org/10.1016/S0924-7963(02)00061-1

Cacho, I., Grimalt, J. O., Pelejero, C., Canals, M., Sierro, F. J., Flores, J. A., & Shackleton, N. J. (1999). Dansgaard-Oeschger and Heinrich event imprints in the Alboran Sea paleotemperatures. *Paleoceanography*, *14*, 698–705. https://doi.org/10.1029/1999PA900044

Cacho, I., Grimalt, J. O., Sierro, F. J., Shackleton, N. J., & Canals, M. (2000). Evidence for enhanced Mediterranean thermohaline circulation during rapid climatic coolings. *Earth and Planetary Science Letters*, *183*, 417–429. https://doi.org/10.1016/S0012-821X(00)00296-X

Capotondi, L., Girone, A., Lirer, F., Bergami, C., Verducci, M., Vallefuoco, M., et al. (2016). Central Mediterranean Mid-Pleistocene paleoclimatic variability and its connection with global climate. *Palaeogeography, Palaeoclimatology, Palaeoecology*, *442*, 72–83. https://doi.org/10.1016/j.palaeo.2015.11.009

Casnedi, R. (1988). La Fossa bradanica: Origine, sedimentazione e migrazione. *Memorie Società Geologica Italiana*, *41*, 439–448.

Cavaleiro, C., Voelker, A. H. L., Stoll, H., Baumann, K. H., Kulhanek, D. K., Naafs, B. D. A., et al. (2018). Insolation forcing of coccolithophore productivity in the North Atlantic during the Middle Pleistocene. *Quaternary Science Reviews*, *191*, 318–336. https://doi.org/10.1016/j.quascirev.2018.05.027

Ciaranfi, N., & D'Alessandro, A. (2005). Overview of the Montalbano Jonico area and section: A proposal for a boundary stratotype for the lower-middle Pleistocene, southern Italy Foredeep. *Quaternary International*, *131*, 5–10. https://doi.org/10.1016/j.quaint.2004.07.003

Ciaranfi, N., Lirer, F., Lirer, L., Lourens, L. J., Maiorano, P., Marino, M., et al. (2010). Integrated stratigraphy and astronomical tuning of the Lower-Middle Pleistocene Montalbano Jonico land section (southern Italy). *Quaternary International*, *210*, 109–120. https://doi.org/10.1016/j.quaint.2009.10.027

Civitarese, G., Gačić, M., Lipizer, M., & Eusebi Borzelli, G. L. (2010). On the impact of the Bimodal Oscillating System (BiOS) on the biogeochemistry and biology of the Adriatic and Ionian seas (Eastern Mediterranean). *Biogeosciences*, *7*, 3987–3997. https://doi.org/10.5194/bg-7-3987-2010

Colmenero-Hidalgo, E., Flores, J. A., Sierro, F. J., Barcena, M. A., Lowemark, L., Schonfeld, J., & Grimalt, J. O. (2004). Ocean surface water response to short-term climate changes revealed by coccolithophores from the Gulf of Cadiz (NE Atlantic) and Alboran Sea (W Mediterranean). *Palaeogeography, Palaeoclimatology, Palaeoecology*, *205*, 317–336. https://doi.org/10.1016/j.palaeo.2003.12.014

Conte, M. H., Sicre, M. A., Rühlemann, C., Weber, J. C., Schulte, S., Schulz-Bull, D., & Blanz, T. (2006). Global temperature calibration of the alkenone unsaturation index (UK′37) in surface waters and comparison with surface sediments. *Geochemistry, Geophysics, Geosystems*, *7*(2), Q02005. https://doi.org/10.1029/2005GC001054

D'Alessandro, A., La Perna, R., & Ciaranfi, N. (2003). Response of macrobenthos to changes in paleoenvironment in the Lower-Middle Pleistocene (Lucania Basin, southern Italy). *Il Quaternario*, *16*, 167–182.

Darling, K. F., Kucera, M., Kroon, D., & Wade, C. M. (2006). A resolution for the coiling direction paradox in *Neogloboquadrina pachyderma*. *Paleoceanography*, *21*(2), PA2011. https://doi.org/10.1029/2005PA001189

Dimiza, M. D., Triantaphyllou, M. V., & Malinverno, E. (2014). New evidence for the ecology of Helicosphaera carteri in polluted coastal environments (Elefsis Bay, Saronikos Gulf, Greece). *Journal of Nannoplankton Research*, *34*, 37–43.

Dittert, N., Baumann, K. H., Bickert, R., Henrich, R., Huber, R., Kinkel, H., & Meggers, H. (1999). Carbonate dissolution in the deep-sea: Methods, quantification and paleoceanographic application. In G. Fischer, & G. Wefer (Eds.), *Use of proxies in paleoceanography: Examples from the South Atlantic* (pp. 255–284). Springer. https://doi.org/10.1007/978-3-642-58646-0_10

D'Ortenzio, F., & Ribera d'Alcalà, M. (2009). On the trophic regimes of the Mediterranean Sea: A satellite analysis. *Biogeosciences*, *6*, 139–148. https://doi.org/10.5194/bg-6-139

Elderfield, H., Ferretti, P., Greaves, M., Crowhurst, S., McCave, I. N., Hodell, D., & Piotrowski, A. M. (2012). Evolution of ocean temperature and ice volume through the mid-Pleistocene climate transition. *Science*, *337*, 704–709. https://doi.org/10.1126/science.1221294

Emanuele, D., Ferretti, P., Palumbo, E., & Amore, F. O. (2015). Sea-surface dynamics and palaeoenvironmental changes in the North Atlantic Ocean (IODP Site U1313) during Marine Isotope Stage 19 inferred from coccolithophore assemblages. *Palaeogeography, Palaeoclimatology, Palaeoecology*, *430*, 104–117. https://doi.org/10.1016/j.palaeo.2015.04.014

Ferretti, P., Crowhurst, S. J., Naafs, B. D. A., & Barbante, C. (2015). The Marine Isotope Stage 19 in the mid-latitude North Atlantic Ocean: Astronomical signature and intra-interglacial variability. *Quaternary Science Reviews*, *108*, 95–110. https://doi.org/10.1016/j.quascirev.2014.10.024

Flores, J.-A., Bárcena, M. A., & Sierro, F. J. (2000). Ocean-surface and wind dynamics in the Atlantic Ocean off Northwest Africa during the last 140,000 years. *Palaeogeography, Palaeoclimatology, Palaeoecology*, *161*, 459–478. https://doi.org/10.1016/s0031-0182(00)00099-7

Flores, J.-A., Filippelli, G. M., Sierro, F. J., & Latimer, J. (2012). The "White Ocean" hypothesis: A late Pleistocene Southern Ocean governed by coccolithophores and driven by phosphorus. *Frontiers in Microbiology*, *3*, 1–13. https://doi.org/10.3389/fmicb.2012.00233

Flores, J.-A., Marino, M., Sierro, F. J., Hodell, D. A., & Charles, C. D. (2003). Calcareous plankton dissolution pattern and coccolithophore assemblages during the last 600 kyr at ODP Site 1089 (Cape Basin, South Atlantic): Paleoceanographic implications. *Palaeogeography, Palaeoclimatology, Palaeoecology*, *196*, 409–426. https://doi.org/10.1016/S0031-0182(03)00467-X

Flores, J.-A., & Sierro, F. J. (1997). Revised technique for calculation of calcareous nannofossil accumulation rates. *Micropaleontology*, *43*, 321–324. https://doi.org/10.2307/1485832

Flores, J.-A., Sierro, F. J., Francés, G., Vázquez, A., & Zamarreño, I. (1997). The last 100,000 years in the western Mediterranean: Sea surface water and frontal dynamics as revealed by Coccolithophores. *Marine Micropaleontology*, *29*, 351–366. https://doi.org/10.1016/s0377-8398(96)00029-1

Gačić, M., Eusebi Borzelli, G. L., Civitarese, G., Cardin, V., & Yari, S. (2010). Can internal processes sustain reversals of the ocean upper circulation? The Ionian Sea example. *Geophysical Research Letters*, *37*, L09608. https://doi.org/10.1029/2010GL043216

Gartner, S. (1988). Paleoceanography of the Mid-Pleistocene. *Marine Micropaleontology*, *13*(1), 23–46. https://doi.org/10.1016/0377-8398(88)90011-4

Giaccio, B., Regattieri, E., Zanchetta, G., Nomade, S., Renne, P. R., Sprain, C. J., et al. (2015). Duration and dynamics of the best orbital analogue to the present interglacial. *Geology*, *43*, 603–606. https://doi.org/10.1130/G36677.1

Gibbs, S. J., Bown, P. R., Murphy, B. H., Sluijs, A., Edgar, K. M., Pälike, H., et al. (2012). Interactive comment on "Scaled biotic disruption during early Eocene global warming events". *Biogeosciences Discussion*, *9*, C618–C620. https://doi.org/10.5194/bg-9-4679-2012

Girone, A., Maiorano, P., Marino, M., & Kucera, M. (2013). Calcareous plankton response to orbital and millennial-scale climate changes across the Middle Pleistocene in the western Mediterranean. *Palaeogeography, Palaeoclimatology, Palaeoecology*, *392*, 105–116. https://doi.org/10.1016/j.palaeo.2013.09.005

Gong, C., & Hollander, D. J. (1999). Evidence for differential degradation of alkenones under contrasting bottom water oxygen conditions: Implication for paleotemperature reconstruction. *Geochimica et Cosmochimica Acta*, *63*(3–4), 405–411. https://doi.org/10.1016/S0016-7037(98)00283-X

González-Lanchas, A., Flores, J. A., Sierro, F. J., Barcena, M. A., Rigual-Hernández, A. S., Oliveira, D., et al. (2020). A New Perspective of the Alboran Upwelling System reconstruction during the Marine Isotope Stage 11: A high-resolution coccolithophore record. *Quaternary Science Reviews*, *245*, 106520. https://doi.org/10.1016/j.quascirev.2020.106520

Grauel, A.-L., Goudeau, M.-L., de Lange, G. J., & Bernasconi, S. M. (2013). Climate of the past 2500 years in the Gulf of Taranto, central Mediterranean Sea: A high-resolution climate reconstruction based on $\delta^{18}O$ and $\delta^{13}C$ of Globigerinoides ruber (white). *The Holocene*, *23*(10), 1440–1446. https://doi.org/10.1177/0959683613493937

Grimalt, J. O., Rullkötter, J., Sicre, M.-A., Summons, R., Farrington, J., Harvey, H. R., et al. (2000). Modifications of the C_{37} alkenone and alkenoate composition in the water colum and sediment: Possible implications for sea surface temperature estimates in paleoceanography. *Geochemistry, Geophysics, Geosystems*, *1*. https://doi.org/10.1029/2000GC000053

Haidar, A. T., & Thierstein, H. R. (2001). Coccolithophore dynamics off Bermuda (N. Atlantic). *Deep-Sea Research Part II: Topical Studies in Oceanography*, *40*, 1925–1956. https://doi.org/10.1016/s0967-0645(00)00169-7

Hammer, Ø., Harper, D. A. T., & Ryan, P. D. (2001). PAST: Paleontological statistics software package for education and data analysis. *Palaeontologia Electronica*, *4*(1), 1–9. Retrieved from http://palaeoelectronica.org/2001_1/past/issue1_01.htm

Hemleben, C., Spindler, M., & Anderson, O. R. (1989). *Modern planktonic foraminifera*. Springer-Verlag.

Herbert, T. D. (2014). Alkenone Paleotemperature Determinations. In H. D. Holland, & K. K. Turekian (Eds.), *Treatise on Geochemistry* (2nd ed., Vol. 8, pp. 399–433). Elsevier. https://doi.org/10.1016/b978-0-08-095975-7.00615-x

Herbert, T. D., Peterson, L. C., & Ng, G. (2015). Evolution of Mediterranean Sea surface temperatures 3.5-1.5 ma: Regional and hemispheric influences. *Earth and Planetary Science Letters*, *409*, 307–318. https://doi.org/10.1016/j.epsl.2014.10.006

Hernández-Almeida, I., Bárcena, M. A., Flores, J. A., Sierro, F. J., Sanchez-Vidal, A., & Calafat, A. (2011). Microplankton response to environmental conditions in the Alboran Sea (Western Mediterranean): One-year sediment trap record. *Marine Micropaleontology*, *78*(1–2), 14–24. https://doi.org/10.1016/j.marmicro.2010.09.005

Hilgen, F. J. (1991). Extension of the astronomically calibrated (polarity) time scale to the Miocene/Pliocene boundary. *Earth and Planetary Science Letters*, *107*(2), 349–368. https://doi.org/10.1016/0012-821X(91)90082-S

Incarbona, A., Di Stefano, E., Patti, B., Pelosi, N., Bonomo, S., Mazzola, S., et al. (2008). Holocene millennial-scale productivity variations in the Sicily Channel (Mediterranean Sea). *Paleoceanography*, *23*. https://doi.org/10.1029/2007PA001581

Incarbona, A., Di Stefano, E., Sprovieri, R., Bonomo, S., Pelosi, N., & Sprovieri, M. (2010). Millennial-scale paleoenvironmental changes in the central Mediterranean during the last interglacial: Comparison with European and North Atlantic records. *Geobios*, *43*(1), 111–122. https://doi.org/10.1016/j.geobios.2009.06.008

Incarbona, A., Martrat, B., Stefano, E. D., Grimalt, J. O., Pelosi, N., Patti, B., & Tranchida, G. (2010). Primary productivity variability on the Atlantic Iberian Margin over the last 70,000 years: Evidence from coccolithophores and fossil organic compounds. *Paleoceanography*, *25*, PA2218. https://doi.org/10.1029/2008PA001709

Incarbona, A., Sprovieri, M., Di Stefano, A., Di Stefano, E., Salvagio Manta, D., Pelosi, N., et al. (2013). Productivity modes in the Mediterranean Sea during Dansgaard-Oeschger (20,000-70,000 yr ago) oscillations. *Palaeogeography, Palaeoclimatology, Palaeoecology*, *392*, 128–137. https://doi.org/10.1016/j.palaeo.2013.09.023

Jordan, R. W., Cros, L., & Young, J. R. (2004). A revised classification scheme for living haptophytes. *Micropaleontology*, *50*, 55–79. https://doi.org/10.2113/50.Suppl_1.55

Klein, B., Roether, W., Kress, N., Manca, B. B., Ribera d'Alcala, M., & Souvermezoglou, E. (2003). Accelerated oxygen consumption in eastern Mediterranean deep waters following the recent changes in thermohaline circulation. *Journal of Geophysical Research*, *108*(C9), 8107. https://doi.org/10.1029/2002JC001454

Kleiven, H., Hall, I. R., McCave, I. N., Knorr, G., & Jansen, E. (2011). Coupled deep-water flow and climate variability in the middle Pleistocene North Atlantic. *Geology*, *39*(4), 343–346. https://doi.org/10.1130/G31651.1

Knappertsbusch, M. (1993). Geographic distribution of living and Holocene coccolithophores in the Mediterranean Sea. *Marine Micropaleontology*, *21*, 219–247. https://doi.org/10.1016/0377-8398(93)90016-q

Konijnendijk, T. Y. M., Ziegler, M., & Lourens, L. J. (2014). Chronological constraints on Pleistocene sapropel depositions from high-resolution geochemical records of ODP Sites 967 and 968. *Newsletters on Stratigraphy*, *47*(3), 263–282. https://doi.org/10.1127/0078-0421/2014/0047

Kontakiotis, G. (2016). Late Quaternary paleoenvironmental reconstruction and paleoclimatic implications of the Aegean Sea (eastern Mediterranean) based on paleoceanographic indexes and stable isotopes. *Quaternary International*, *401*, 28–42. https://doi.org/10.1016/j.quaint.2015.07.039

Laskar, J., Robutel, P., Joutel, F., Gastineau, M., Correia, A. C. M., & Levrard, B. (2004). A long-term numerical solution for the insolation quantities of the Earth. *Astronomy & Astrophysics*, *428*, 261–285. https://doi.org/10.1051/0004-6361:20041335

Lionello, P. (2012). *The climate of the Mediterranean region, from the past to the future*. Elsevier. https://doi.org/10.1016/C2011-0-06210-5

Lionello, P., Malanotte-Rizzoli, P., & Boscolo, R. (2006). *Mediterranean climate variability*. Elsevier.

López-Otálvaro, G.-E., Flores, J. A., Sierro, F. J., & Cacho, I. (2008). Variations in coccolithophorid production in the Eastern Equatorial Pacific at ODP Site 1240 over the last seven glacial-interglacial cycles. *Marine Micropaleontology*, *69*, 52–69. https://doi.org/10.1016/j.marmicro.2007.11.009

López-Otálvaro, G.-E., Flores, J. A., Sierro, F. J., Cacho, I., Grimalt, J.-O., Michel, E., et al. (2009). Late Pleistocene palaeoproductivity patterns during the last climatic cycle in the Guyana Basin as revealed by calcareous nannoplankton. *eEarth*, *4*, 1–13. https://doi.org/10.5194/ee-4-1-2009

Lourens, L. J. (2004). Revised tuning of Ocean Drilling Program Site 964 and KC01B (Mediterranean) and implications for the $\delta^{18}O$, tephra, calcareous nannofossil, and geomagnetic reversal chronologies of the past 1.1 Myr. *Paleoceanography*, *19*, PA3010. https://doi.org/10.1029/2003PA000997

Ludwig, W., Dumont, E., Meybeck, M., & Heussner, S. (2009). River discharges of water and nutrients to the Mediterranean and Black Sea: Major drivers for ecosystem changes during past and future decades. *Progress in Oceanography*, *80*, 199–217. https://doi.org/10.1016/j.pocean.2009.02.001

Macias, D. M., Garcia-Gorriz, E., & Stips, A. (2015). Productivity changes in the Mediterranean Sea for the twenty-first century in response to changes in the regional atmospheric forcing. *Frontiers in Marine Science*, *2*, 79. https://doi.org/10.3389/fmars.2015.00079

Madureira, L. A. S., Conte, M. H., & Eglinton, G. (1995). Early diagenesis of lipid biomarker compounds in North Atlantic sediments. *Paleoceanography*, *10*(3), 627–642. https://doi.org/10.1029/94PA03299

Maiorano, P., Bertini, A., Capolongo, D., Eramo, G., Gallicchio, S., Girone, A., et al. (2016). Climate signatures through the Marine Isotope Stage 19 in the Montalbano Jonico section (Southern Italy): A land-sea perspective. *Palaeogeography, Palaeoclimatology, Palaeoecology*, *461*, 341–361. https://doi.org/10.1016/j.palaeo.2016.08.029

Maiorano, P., Capotondi, L., Ciaranfi, N., Girone, A., Lirer, F., Marino, M., et al. (2010). Vrica-Crotone and Montalbano Jonico sections: A potential unit-stratotype of the Calabrian Stage. *Episodes*, *33*, 218–233. https://doi.org/10.18814/epiiugs/2010/v33i4/001

Maiorano, P., Marino, M., Balestra, B., Flores, J. A., Hodell, D. A., & Rodrigues, T. (2015). Coccolithophore variability from the Shackleton Site (IODP Site U1385) through MIS 16–10. *Global and Planetary Change*, *133*, 35–48. https://doi.org/10.1016/j.gloplacha.2015.07.009

Maiorano, P., Marino, M., & De Lange, G. J. (2019). Dynamic surface-water alterations during sapropel S1 preserved in high-resolution shallow-water sediments of Taranto Gulf, central Mediterranean. *Palaeogeography, Palaeoclimatology, Palaeoecology*, *534*, 109340. https://doi.org/10.1016/j.palaeo.2019.109340

Maiorano, P., Tarantino, F., Marino, M., & De Lange, G. J. (2013). Paleoenvironmental conditions at Core KC01B (Ionian Sea) through MIS 13-9: Evidence from calcareous nannofossil assemblages. *Quaternary International*, *288*, 97–111. https://doi.org/10.1016/j.quaint.2011.12.007

Malanotte-Rizzoli, P., Manca, B., Ribera D'Alcalà, M., Theocharis, A., Bergamasco, A., Bregant, D., et al. (1997). A synthesis of the Ionian Sea hydrography, circulation and water mass pathway during POEM-Phase I. *Progress in Oceanography*, *39*(3), 153–204. https://doi.org/10.1016/S0079-6611(97)00013-X

Malinverno, E., Prahl, F. G., Popp, B. N., & Ziveri, P. (2008). Alkenone abundance and its relationship to the coccolithophore assemblage in Gulf of California surface waters. *Deep-Sea Research I: Oceanographic Research Papers*, *55*, 1118–1130. https://doi.org/10.1016/j.dsr.2008.04.007

Malinverno, E., Triantaphyllou, M. V., Stavrakakis, S., Ziveri, P., & Lykousis, V. (2009). Seasonal and spatial variability of coccolithophore export production at the southwestern margin of Crete (eastern Mediterranean). *Marine Micropaleontology*, *71*(3–4), 131–147. https://doi.org/10.1016/j.marmicro.2009.02.002

Malinverno, E., Ziveri, P., & Corselli, C. (2003). Coccolithophorid distribution in the Ionian Sea and its relationship to eastern Mediterranean circulation during late fall to early winter 1997. *Journal of Geophysical Research*, *108*, 2156–2202. https://doi.org/10.1029/2002JC001346

Mallo, M., Ziveri, P., Mortyn, P. G., Schiebel, R., & Grelaud, M. (2017). Low planktic foraminiferal diversity and abundance observed in a spring 2013 west–east Mediterranean Sea plankton tow transect. *Biogeosciences*, *14*, 2245–2266. https://doi.org/10.5194/bg-14-2245-2017

Mangili, C., Brauer, A., Plessen, B., & Moscariello, A. (2007). Centennial-scale oscillations in oxygen and carbon isotopes of endogenic calcite from a 15,500 varve year record of the Pànico interglacial. *Quaternary Science Reviews*, *26*(13–14), 1725–1735. https://doi.org/10.1016/j.quascirev.2007.04.012

Marino, M., Aiello, G., Barra, D., Bertini, A., Gallicchio, S., & Girone, A. (2016). The Montalbano Jonico section (South Italy) as a reference for the Early/Middle Pleistocene boundary. *Alpine and Mediterranean Quaternary*, *29*(1), 45–57.

Marino, M., Bertini, A., Ciaranfi, N., Aiello, G., Barra, D., Gallicchio, S., et al. (2015). Paleoenvironmental and climatostratigraphic insights for Marine Isotope Stage 19 (Pleistocene) at the Montalbano Jonico section, South Italy. *Quaternary International*, *383*, 104–115. https://doi.org/10.1016/j.quaint.2015.01.043

Marino, M., Girone, A., Gallicchio, S., Herbert, T., Addante, M., Bazzicalupo, P., et al. (2020). Climate variability during MIS 20-18 as recorded by alkenone-SST and calcareous plankton in the Ionian Basin (central Mediterranean). *Palaeogeography, Palaeoclimatology, Palaeoecology*, *560*, 110027. https://doi.org/10.1016/j.palaeo.2020.110027

Marino, M., Girone, A., Maiorano, P., Di Renzo, R., Piscitelli, A., & Flores, J.-A. (2018). Calcareous plankton and the mid-Brunhes climate variability in the Alboran Sea (ODP Site 977). *Palaeogeography, Palaeoclimatology, Palaeoecology*, *508*, 91–106. https://doi.org/10.1016/j.palaeo.2018.07.023

Marino, M., Maiorano, P., & Flower, B. P. (2011). Calcareous nannofossil changes during the Mid-Pleistocene revolution: Paleoecologic and paleoceanographic evidence from North Atlantic Site 980/981. *Palaeogeography, Palaeoclimatology, Palaeoecology*, *306*(1–2), 58–69. https://doi.org/10.1016/j.palaeo.2011.03.028

Marino, M., Maiorano, P., Tarantino, F., Voelker, A., Capotondi, L., Girone, A., et al. (2014). Coccolithophores as proxy of seawater changes at orbital- to-millennial scale during middle Pleistocene Marine Isotope Stages 14–9 in North Atlantic core MD01-2446. *Paleoceanography*, *29*, 518–532. https://doi.org/10.1002/2013PA002574

Marlowe, I. T., Brassell, S. C., Eglinton, G., & Green, J. C. (1990). Long-chain alkenones and alkyl alkenoates and the fossil coccolith record of marine sediments. *Chemical Geology*, *88*(3–4), 349–375. https://doi.org/10.1016/0009-2541(90)90098-R

Marlowe, I. T., Green, J. C., Neal, A. C., Brassell, S. C., Eglinton, G., & Course, P. A. (1984). Long chain (n-C37–C39) alkenones in the Prymnesiophyceae. Distribution of alkenones and other lipids and their taxonomic significance. *British Phycological Journal*, *19*(3), 203–216. https://doi.org/10.1080/00071618400650221

Martinez-Sanchez, M., Flores, J.-A., Palumbo, E., Alonso-Garciac, M., Sierro, F. J., & Amore, F. O. (2019). Reconstruction of surface water dynamics in the North Atlantic during the Mid-Pleistocene (~540–400 ka), as inferred from coccolithophores and planktonic foraminifera. *Marine Micropaleontology*, *152*, 101730. https://doi.org/10.1016/j.marmicro.2019.03.002

McIntyre, A., & Bé, A. H. W. (1967). Modern coccolithophores of the Atlantic Ocean—I. Placolith and cyrtoliths. *Deep-Sea Research and Oceanographic Abstracts*, *14*, 561–597. https://doi.org/10.1016/0011-7471(67)90065-4

McIntyre, A., & Molfino, B. (1996). Forcing of Atlantic equatorial and subpolar millennial cycles by precession. *Science*, *274*(5294), 1867–1870. https://doi.org/10.1126/science.274.5294.1867

Mejía, L. M., Ziveri, P., Cagnetti, M., Bolton, C., Zahn, R., Marino, G., et al. (2014). Effects of mid latitude westerlies on the paleoproductivity at the Agulhas Bank slope during the penultimate glacial cycle: Evidence from coccolith Sr/Ca ratios. *Paleoceanography*, *29*, 697–714. https://doi.org/10.1002/2013PA002589

Melki, T., Kallel, N., Jorissen, F. J., Guichard, F., Dennielou, B., Bern, S., et al. (2009). Abrupt climate change, sea surface salinity and paleoproductivity in the western Mediterranean Sea (Gulf of Lion) during the last 28 kyr. *Palaeogeography, Palaeoclimatology, Palaeoecology*, *279*, 96–113. https://doi.org/10.1016/j.palaeo.2009.05.005

Milligan, T. G., & Cattaneo, A. (2007). Sediment dynamics in the western Adriatic Sea: From transport to stratigraphy. *Continental Shelf Research*, *27*, 287–295. https://doi.org/10.1016/j.csr.2006.11.001

Milner, A. M., Collier, R. E. L., Roucoux, K. H., Müller, U. C., Pross, J., Kalaitzidis, S., et al. (2012). Enhanced seasonality of precipitation in the Mediterranean during the early part of the Last Interglacial. *Geology*, *40*, 919–922. https://doi.org/10.1130/G33204.1

Molfino, B., & McIntyre, A. (1990a). Nutricline variation in the equatorial Atlantic coincident with the Younger Dryas. *Paleoceanography*, *5*, 997–1008. https://doi.org/10.1029/PA005i006p00997

Molfino, B., & McIntyre, A. (1990b). Precessional forcing of nutricline dynamics in the equatorial Atlantic. *Science*, *249*, 766–769. https://doi.org/10.1126/science.249.4970.766

Moreno, A., Cacho, I., Canals, M., Grimalt, J. O., Sánchez-Goñi, M. F., Shackleton, N., & Sierro, F. J. (2005). Links between marine and atmospheric processes oscillating on a millennial time-scale. A multi-proxy study of the last 50,000 yr from the Alboran Sea (Western Mediterranean Sea). *Quaternary Science Reviews*, *24*(14–15), 1623–1636. https://doi.org/10.1016/j.quascirev.2004.06.018

Moreno, A., Cacho, I., Canals, M., Grimalt, J. O., & Sanchez-Vidal, A. (2004). Millennial-scale variability in the productivity signal from the Alboran Sea record, Western Mediterranean Sea. *Palaeogeography, Palaeoclimatology, Palaeoecology*, *211*(3–4), 205–219. https://doi.org/10.1016/j.palaeo.2004.05.007

Moscariello, A., Ravazzi, C., Brauer, A., Mangili, C., Chiesa, S., Rossi, S., et al. (2000). A long lacustrine record from the Piànico-Sèllere basin (Middle-Late Pleistocene, Nothern Italy). *Quaternary International*, *73/74*, 47–68. https://doi.org/10.1016/S1040-6182(00)00064-1

Müller, P. J., Kirst, G., Ruhland, G., Von Storch, I., & Rosell-Melé, A. (1998). Calibration of the alkenone paleotemperature index Uk'37 based on core-tops from the eastern South Atlantic and the global ocean (60°N-60°S). *Geochimica et Cosmochimica Acta*, *62*(10), 1757–1772. https://doi.org/10.1016/s0016-7037(98)00097-0

Nomade, S., Bassinot, F., Marino, M., Simon, Q., Dewilde, F., Maiorano, P., et al. (2019). High-resolution foraminifer stable isotope record of MIS 19 at Montalbano Jonico, southern Italy: A window into Mediterranean climatic variability during a low-eccentricity interglacial. *Quaternary Science Reviews*, *205*, 106–125. https://doi.org/10.1016/j.quascirev.2018.12.008

Okada, H. (1992). Biogeographic control of modern nannofossil assemblages in surface sediments of Ise Bay, Mikawa Bay and Kumano-nada, off coast of Central Japan. *Memorie di Scienze Geologiche*, *43*, 431–449.

Oviedo, A. M., Ziveri, P., Álvarez, M., & Tanhua, T. (2015). Is coccolithophore distribution in the Mediterranean Sea related to seawater carbonate chemistry? *Ocean Science*, *11*, 13–32. https://doi.org/10.5194/os-11-13-2015

Oviedo, A. M., Ziveri, P., & Gazeau, F. (2017). Coccolithophore community response to increasing pCO_2 in Mediterranean oligotrophic waters. *Estuarine, Coastal and Shelf Science*, *186*, 58–71. https://doi.org/10.1016/j.ecss.2015.12.007

Palumbo, E., Flores, J. A., Perugia, C., Petrillo, Z., Voelker, A. H. L., & Amore, F. O. (2013). Millennial scale coccolithophore paleoproductivity and surface water changes between 445 and 360 ka (Marine Isotope Stages 12/11) in the Northeast Atlantic. *Palaeogeography, Palaeoclimatology, Palaeoecology*, *383–384*, 27–41. https://doi.org/10.1016/j.palaeo.2013.04.024

Pérez-Folgado, M., Sierro, F. J., Flores, J. A., Cacho, I., Grimalt, J. O., Zahn, R., & Shackleton, N. (2003). Western Mediterranean planktonic foraminifera events and millennial climatic variability during the last 70 kyr. *Marine Micropaleontology*, *48*(1–2), 49–70. https://doi.org/10.1016/S0377-8398(02)00160-3

Petrosino, P., Jicha, B. R., Mazzeo, F. C., Ciaranfi, N., Girone, A., Maiorano, P., & Marino, M. (2015). The Montalbano Jonico marine succession: An archive for distal tephra layers at the Early-Middle Pleistocene boundary in southern Italy. *Quaternary International*, *383*, 89–103. https://doi.org/10.1016/j.quaint.2014.10.049

Plancq, J. (2015). *Identification Des Producteurs d'alcénones dans le Register Sédimentaire du Cénozoïque: Implications Pour l'utilisation Des Proxys de Paléo-température (U37k') et de Paléo-pCO_2* Ph.D. Thesis (Vol. 1). L'universite Claude Bernard Lyon.

Plancq, J., Grossi, V., Henderiks, J., Simon, L., & Mattioli, E. (2012). Alkenone producers during late Oligocene–early Miocene revisited. *Paleoceanography*, *27*, PA1202. https://doi.org/10.1029/2011PA002164

Pol, K., Masson-Delmotte, V., Johnsen, S., Bigler, M., Cattani, O., Durand, G., et al. (2010). New MIS 19 EPICA Dome C high resolution deuterium data: Hints for a problematic preservation of climate variability in the "oldest ice". *Earth and Planetary Science Letters*, *298*(1–2), 95–103. https://doi.org/10.1016/j.epsl.2010.07.030

Poulain, P.-M. (2001). Adriatic Sea surface circulation as derived from drifter data between 1990 and 1999. *Journal of Marine Systems*, *29*, 3–32. https://doi.org/10.1016/S0924-7963(01)00007-0

Prahl, F. G., Collier, R. B., Dymond, J., Lyle, M., & Sparrow, M. A. (1993). A biomarker perspective on prymnesiophyte productivity in the northeast Pacific Ocean. *Deep Sea Research Part I: Oceanographic Research Papers*, *40*, 2061–2076. https://doi.org/10.1016/0967-0637(93)90045-5

Prahl, F. G., De Lange, G. J., Lyle, M., & Sparrow, M. A. (1989). Post-depositional stability of long-chain alkenones under contrasting redox conditions. *Nature*, *341*, 434–437. https://doi.org/10.1038/340301a010.1038/341434a0

Prahl, F. G., Pilskaln, C., & Sparrow, M. (2001). Seasonal record for alkenones in sedimentary particles from the Gulf of Maine. *Deep Sea Research Part I: Oceanographic Research Papers*, *48*, 515–528. https://doi.org/10.1016/S0967-0637(00)00057-1

Prahl, F. G., & Wakeham, S. G. (1987). Calibration of unsaturation patterns in long-chain ketone compositions for palaeotemperature assessment. *Nature*, *330*, 367–369. https://doi.org/10.1038/330367a0

Pujol, C., & Vergnaud-Grazzini, C. (1995). Distribution patterns of live planktic foraminifers as related to regional hydrography and productive systems of the Mediterranean Sea. *Marine Micropaleontology*, *25*(2–3), 187–217. https://doi.org/10.1016/0377-8398(95)00002-I

Quivelli, O. (2020). *Coccolithophores and biomarkers as paleoclimatic and paleoceanographic indicators during Marine Isotope Stage 20-18* Ph.D. Thesis (p. 210). Università degli Studi di Bari.

Quivelli, O., Marino, M., Rodrigues, T., Girone, A., Maiorano, P., Abrantes, F., et al. (2020). Surface and deep water variability in the Western Mediterranean (ODP Site 975) during insolation cycle 74: High-resolution calcareous plankton and molecular biomarker signals. *Palaeogeography, Palaeoclimatology, Palaeoecology*, *542*, 109583. https://doi.org/10.1016/j.palaeo.2019.109583

Regattieri, E., Giaccio, B., Mannella, G., Zanchetta, G., Nomade, S., Tognarelli, A., et al. (2019). Frequency and dynamics of millennial-scale variability during Marine Isotope Stage 19: Insights from the Sulmona Basin (central Italy). *Quaternary Science Reviews*, *214*, 28–43. https://doi.org/10.1016/j.quascirev.2019.04.024

Regattieri, E., Giaccio, B., Zanchetta, G., Drysdale, R. N., Galli, P., Peronace, E., et al. (2015). Hydrological variability over Apennine during the Early Late Glacial precession minimum, as revealed by a stable isotope record from Sulmona basin, central Italy. *Journal of Quaternary Science*, *30*, 19–31. https://doi.org/10.1002/jqs.2755

Richon, C., Dutay, J.-C., Bopp, L., Le Vu, B., Orr, J. C., Somot, S., & Dulac, F. (2019). Biogeochemical response of the Mediterranean Sea to the transient SRES-A2 climate change scenario. *Biogeosciences*, *16*, 135–165. https://doi.org/10.5194/bg-16-135-2019

Rickaby, R. E. M., Elderfield, H., Roberts, N., Hillenbrand, C.-D., & Mackensen, A. (2010). Evidence for elevated alkalinity in the glacial Southern Ocean. *Paleoceanography*, *25*. https://doi.org/10.1029/2009PA001762

Rigual-Hernández, A. S., Sierro, F. J., Bárcena, M. A., Flores, J. A., & Heussner, S. (2012). Seasonal and interannual changes of planktic foraminiferal fluxes in the Gulf of Lions (NW Mediterranean) and their implications for paleoceanographic studies: Two 12-year sediment trap records. *Deep-Sea Research Part I: Oceanographic Research Papers*, *66*, 26–40. https://doi.org/10.1016/j.dsr.2012.03.011

Robinson, A. R., Sellshop, J., Warn-Varnas, A., Leslie, W. G., Lozano, C. J., Haley, P. J., Jr, et al. (1999). The Atlantic Ionian stream. *Journal of Marine Systems*, *20*(1–4), 129–156. https://doi.org/10.1016/S0924-7963(98)00079-7

Rodrigues, T., Alonso-Garcia, M., Hodell, D. A., Rufino, M., Naughton, F., Grimalt, J. O., et al. (2017). A 1-Ma record of sea surface temperature and extreme cooling events in the North Atlantic: A perspective from the Iberian margin. *Quaternary Science Reviews*, *172*, 118–130. https://doi.org/10.1016/j.quascirev.2017.07.004

Rohling, E. J., Cane, T. R., Cooke, S., Sprovieri, M., Bouloubassi, I., Emeis, K. C., et al. (2002). African monsoon variability during the previous interglacial maximum. *Earth and Planetary Science Letters*, *202*, 61–75. https://doi.org/10.1016/S0012-821X(02)00775-6

Rohling, E. J., Jorissen, F. J., & De Stigter, H. C. (1997). 200-year interruption of Holocene sapropel formation in the Adriatic Sea. *Journal of Micropalaeontology*, *16*(2), 97–108. https://doi.org/10.1144/jm.16.2.97

Rohling, E. J., Marino, G., & Grant, K. (2015). Mediterranean climate and oceanography, and the periodic development of anoxic events (sapropels). *Earth-Science Reviews*, *143*, 62–97. https://doi.org/10.1016/j.earscirev.2015.01.008

Rontani, J.-F., & Volkman, J. K. (2005). Lipid characterization of coastal hypersaline cyanobacterial mats from the Camargue (France). *Organic Geochemistry*, *36*, 251–272. https://doi.org/10.1016/j.orggeochem.2004.07.017

Rossi, S. (2003). *Etude pollinique de la sequence lacustre Pléistocene de Piànico-Sèllere (Italie)* Ph.D. Thesis. Universitè de Droit d'Economie et des Sciences d'Aix Marseille III.

Rossignol-Strick, M. (1985). Mediterranean Quaternary sapropels, an immediate response of the African monsoon to variation of insolation. *Palaeogeography, Palaeoclimatology, Palaeoecology*, *49*(3–4), 237–263. https://doi.org/10.1016/0031-0182(85)90056-2

Rossignol-Strick, M., Nesteroff, W., Olive, P., & Vergnaud-Grazzini, C. (1982). After the deluge: Mediterranean stagnation and sapropel formation. *Nature*, *295*, 105–110. https://doi.org/10.1038/295105a0

Saavedra-Pellitero, M., Baumann, K.-H., Ullermann, J., & Lamy, F. (2017). Marine isotope stage 11 in the pacific sector of the Southern Ocean; a coccolithophore perspective. *Quaternary Science Reviews*, *158*, 1–14. https://doi.org/10.1016/j.quascirev.2016.12.020

Saavedra-Pellitero, M., Flores, J.-A., Baumann, K.-H., & Sierro, F. J. (2010). Coccolith distribution patterns in surface sediments of equatorial and southeastern Pacific Ocean. *Geobios*, *43*, 131–149. https://doi.org/10.1016/j.geobios.2009.09.004

Saavedra Pellitero, M., Flores, J.-A., Lamy, F., Sierro, F. J., & Cortina, A. (2011). Coccolithophore estimates of paleotemperature and paleoproductivity changes in the southeast Pacific over the past ~27 ka. *Paleoceanography*, *26*. https://doi.org/10.1029/2009PA001824

Sachs, J. P., Schneider, R. R., Eglinton, T. I., Freeman, K. H., Ganssen, G., McManus, J. F., & Oppo, D. W. (2000). Alkenones as paleoceanographic proxies. *Geochemistry, Geophysics, Geosystems*, *1*(11). https://doi.org/10.1029/2000GC000059

Sánchez-Goñi, M. F., Rodrigues, T., Hodell, D. A., Polanco-Martínez, J. M., Alonso-García, M., Hernández-Almeida, I., et al. (2016). Tropically-driven climate shifts in southwestern Europe during MIS 19, a low eccentricity interglacial. *Earth and Planetary Science Letters*, *448*, 81–93. https://doi.org/10.1016/j.epsl.2016.05.018

Schiebel, R., Bijma, J., & Hemleben, C. (1997). Population dynamics of the planktic foraminifer *Globigerina bulloides* from the eastern North Atlantic. *Deep-Sea Research Part I: Oceanographic Research Papers*, *44*(9–10), 1701–1713. https://doi.org/10.1016/s0967-0637(97)00036-8

Schiebel, R., & Hemleben, C. (2005). Modern planktic foraminifera. *Paläontologische Zeitschrift*, *79*(1), 135–148. https://doi.org/10.1007/bf03021758

Schwab, C., Kinkel, H., Weinelt, M., & Repschlger, J. (2012). Coccolithophore paleoproductivity and ecology response to deglacial and Holocene changes in the Azores Current System. *Paleoceanography*, *27*. https://doi.org/10.1029/2012PA002281

Sellschopp, J., & Álvarez, A. (2003). Dense low-salinity outflow from the Adriatic Sea under mild (2001) and strong (1999) winter conditions. *Journal of Geophysical Research*, *108*(C9), 8104. https://doi.org/10.1029/2002JC001562

Sicre, M. A., Ternois, Y., Paterne, M., Boireau, A., Beaufort, L., Martinez, P., & Bertrand, P. (2000). Biomarker stratigraphic records over the last 150 k years off the NW African coast at 25°N. *Organic Geochemistry*, *31*, 577–588. https://doi.org/10.1016/s0146-6380(00)00021-8

Sierro, F. J., Hodell, D. A., Curtis, J. H., Flores, J. A., Reguera, I., Colmenero-Hidalgo, E., et al. (2005). Impact of iceberg melting on Mediterranean thermohaline circulation during Heinrich events. *Paleoceanography*, *20*, PA2019. https://doi.org/10.1029/2004PA001051

Simon, Q., Bourlès, L. D., Bassinot, F., Nomade, S., Marino, M., Ciaranfi, N., et al. (2017). Authigenic $^{10}Be/^{9}Be$ ratio signature of the Matuyama-Brunhes boundary in the Montalbano Jonico marine succession. *Earth and Planetary Science Letters*, *460*, 255–267. https://doi.org/10.1016/j.epsl.2016.11.052

Sinninghe Damsté, J. S., Rijpstra, W. I. C., & Reichart, G.-J. (2002). The influence of oxic degradation on the sedimentary biomarker record II. Evidence from Arabian Sea sediments. *Geochimica et Cosmochimica Acta*, *66*(15), 2737–2754. https://doi.org/10.1016/S0016-7037(02)00865-7

Sprovieri, R., Di Stefano, E., Incarbona, A., & Gargano, M. E. (2003). A high-resolution record of the last deglaciation in the Sicily Channel based on foraminifera and calcareous nannofossil quantitative distribution. *Palaeogeography, Palaeoclimatology, Palaeoecology*, *202*(1–2), 119–142. https://doi.org/10.1016/S0031-0182(03)00632-1

Sprovieri, R., Di Stefano, E., Incarbona, A., & Oppo, D. W. (2006). Suborbital climate variability during Marine Isotopic Stage 5 in the central Mediterranean Basin: Evidence from calcareous plankton. *Quaternary Science Reviews*, *25*(17–18), 2332–2342. https://doi.org/10.1016/j.quascirev.2006.01.035

Stefanelli, S. (2003). Benthic foraminiferal assemblages as tools for paleoenvironmental reconstruction of the early-middle Pleistocene Montalbano Jonico composite section. *Bollettino Società Paleontologica Italiana*, *42*, 281–299.

Steinmetz, J. C. (1994). Sedimentation of coccolithophores. In A. Winter, & W. G. Siesser (Eds.), *Coccolithophores* (pp. 179–197). Cambridge University Press.

Stolz, K., & Baumann, K. H. (2010). Changes in palaeoceanography and palaeoecology during Marine Isotope Stage (MIS) 5 in the eastern North Atlantic (ODP Site 980) deduced from calcareous nannoplankton observations. *Palaeogeography, Palaeoclimatology, Palaeoecology*, *292*(1–2), 295–305. https://doi.org/10.1016/j.palaeo.2010.04.002

Takahashi, K., & Okada, H. (2000). Environmental control on the biogeography of modern coccolithophores in the southeastern Indian Ocean offshore of Western Australia. *Marine Micropaleontology*, *39*, 73–86. https://doi.org/10.1016/S0377-8398(00)00015-3

Tangunan, D., Baumann, K.-H., Pätzold, J., Henrich, R., Kucera, M., De Pol-Holz, R., & Groeneveld, J. (2017). Insolation forcing of coccolithophore productivity in the western tropical Indian Ocean over the last two glacial-interglacial cycles. *Paleoceanography*, *32*, 692–709. https://doi.org/10.1002/2017PA003102

Tangunan, D., Berke, M. A., Cartagena-Sierra, A., Flores, J.-A., Gruetzner, J., Jiménez-Espejo, F., et al. (2021). Strong glacial-interglacial variability in upper ocean hydrodynamics, biogeochemistry, and productivity in the southern Indian Ocean. *Communication Earth & Environment*, *2*, 2–80. https://doi.org/10.1038/s43247-021-00148-0

Taricco, C., Vivaldo, G., Alessio, S., Rubinetti, S., & Mancuso, S. (2015). A high-resolution _^{18}O record and Mediterranean climate variability. *Climate of the Past*, *11*, 509–522. https://doi.org/10.5194/cp-11-509-2015

Tierney, J. E., & Tingley, M. P. (2018). BAYSPLINE: A new calibration for the alkenone paleothermometer. *Paleoceanography and Paleoclimatology*, *33*(3), 281–301. https://doi.org/10.1002/2017PA003201

Toti, F., Bertini, A., Girone, A., Marino, M., Maiorano, P., Bassinot, F., et al. (2020). Marine and terrestrial climate variability in the western Mediterranean Sea during marine isotope stages 20 and 19. *Quanternary Science Reviews*, *243*, 106486. https://doi.org/10.1016/j.quascirev.2020.106486

Toucanne, S., Minto'o, C. M. A., Fontanier, C., Bassetti, M.-A., Jorry, S. J., & Jouet, G. (2015). Tracking rainfall in the northern Mediterranean borderlands during sapropel deposition. *Quaternary Science Reviews*, *129*, 178–195. https://doi.org/10.1016/j.quascirev.2015.10.016

Triantaphyllou, M. V., Antonarakou, A., Dimiza, M. D., & Anagnostou, C. (2010). Calcareous nannofossil and planktonic foraminiferal distributional patterns during deposition of sapropels S6, S5 and S1 in the Libyan Sea (Eastern Mediterranean). *Geo-Marine Letters*, *30*, 1–13. https://doi.org/10.1007/s00367-009-0145-7

Turchetto, M., Boldrin, A., Langone, L., Miserocchi, S., Tesi, T., & Foglini, F. (2007). Particle transport in the Bari Canyon (southern Adriatic Sea). *Marine Geology*, *246*, 231–247. https://doi.org/10.1016/j.margeo.2007.02.007

Tzedakis, P. C. (2007). Seven ambiguities in the Mediterranean palaeoenvironmental narrative. *Quaternary Science Reviews*, *26*, 2042–2066. https://doi.org/10.1016/j.quascirev.2007.03.014
Tzedakis, P. C., Channell, J. E. T., Hodell, D. A., Kleiven, H. F., & Skinner, L. C. (2012). Determining the natural length of the current interglacial. *Nature Geoscience*, *5*, 138–141. https://doi.org/10.1038/NGEO1358
Vilibić, I., & Orlić, M. (2002). Adriatic water masses, their rates of formation and transport through the Otranto Strait. *Deep-Sea Research Part I: Oceanographic Research Papers*, *49*, 1321–1340. https://doi.org/10.1016/S0967-0637(02)00028-6
Villanueva, J., Calvo, E., Pelejero, C., Grimalt, J. O., Boelaert, A., & Labeyrie, L. (2001). A latitudinal productivity band in the central North Atlantic over the last 270 kyr: An alkenone perspective. *Paleoceanography*, *16*, 617–626. https://doi.org/10.1029/2000PA000543
Villanueva, J., Flores, J. A., & Grimalt, J. O. (2002). A detailed comparison of the U37k′ and coccolith records over the past 290 k years; implications to the alkenone paleotemperature method. *Organic Geochemistry*, *33*, 897–905. https://doi.org/10.1016/s0146-6380(02)00067-0
Volkman, J. K., Barrett, S. M., Blackburn, S. I., & Sikes, E. L. (1995). Alkenones in *Gephyrocapsa oceanica*: Implications for studies of paleoclimate. *Geochimica et Cosmochimica Acta*, *59*(3), 513–520. https://doi.org/10.1016/0016-7037(95)00325-T
Volkman, J. K., Eglinton, G., Corner, E. D. S., & Forsberg, T. E. V. (1980). Long-chain alkenes and alkenones in the marine coccolithophorid *Emiliania huxleyi*. *Phytochemistry*, *19*(12), 2619–2622. https://doi.org/10.1016/S0031-9422(00)83930-8
Wagner, B., Vogel, H., Francke, A., Friedrich, T., Donders, T., Lacey, J. H., et al. (2019). Mediterranean winter rainfall in phase with African monsoons during the past 1.36 million years. *Nature*, *573*, 256–260. https://doi.org/10.1038/s41586-019-1529-0
Weaver, P. P. E., Chapman, M. R., Eglinton, G., Zhao, M., Rutledge, D., & Read, G. (1999). Combined coccolith, foraminiferal, and biomarker reconstruction of paleoceanographic conditions over the past 120 kyr in the northern North Atlantic (59°N, 23°W). *Paleoceanography*, *14*, 336–349. https://doi.org/10.1029/1999PA900009
Winter, A., Jordan, R. W., & Roth, P. H. (1994). Biogeography of living coccolithophores in ocean waters. In A. Winter, & W. G. Siesser (Eds.), *Coccolithophores* (pp. 161–178). Cambridge University Press.
Wright, A. K., & Flower, B. P. (2002). Surface and deep ocean circulation in subpolar North Atlantic during the mid-Pleistocene revolution. *Paleoceanography*, *17*. https://doi.org/10.1029/2002PA000782
Young, J. R. (1994). Functions of coccoliths. In A. Winter, & W. G. Siesser (Eds.), *Coccolithophores* (pp. 63–82). Cambridge University Press.
Young, J. R., Geisen, M., Cros, L., Kleijne, A., Sprengel, C., Probert, I., & Østergaard, J. (2003). A guide to extant coccolithophore taxonomy. *Journal of Nannoplankton Research*, *1*(Special Issue), 1–125.
Zachariasse, W. J., Jorissen, F. J., Perissoratis, C., Rohling, E. J., & Tsapralis, V. (1997). Late Quaternary foraminiferal changes and the nature of sapropel S1 in Skopelos Basin. In *Proceeding of the 5th Hellenic Symposium on Oceanography and Fisheries* (pp. 391–394). http://symposia.ath.hcmr.gr/oldver/symposia5/391.pdf
Ziveri, P., Baumann, K.-H., Boeckel, B., Bollmann, J., & Young, Y. R. (2004). Biogeography of selected Holocene coccoliths in the Atlantic Ocean. In H. R. Thierstein, & Y. R. Young (Eds.), *Coccolithophores* (pp. 403–428). Springer. https://doi.org/10.1007/978-3-662-06278-4_15
Ziveri, P., Thunell, R. C., & Rio, D. (1995). Export production of coccolithophores in an upwelling region: Results from San Pedro Basin, Southern California Borderlands. *Marine Micropaleontology*, *24*, 335–358. https://doi.org/10.1016/0377-8398(94)00017-H

References From the Supporting Information

Ausín, B., Zúñiga, D., Flores, J. A., Cavaleiro, C., Froján, M., Villacieros-Robineau, N., et al. (2018). Spatial and temporal variability in coccolithophore abundance and distribution in the NW Iberian coastal upwelling system. *Biogeosciences*, *15*, 245–262. https://doi.org/10.5194/bg-15-245-2018
Becker, K. W., Lipp, J. S., Versteegh, G. J. M., Wörmer, L., & Hinrichs, K.-U. (2015). Rapid and simultaneous analysis of three molecular sea surface temperature proxies and application to sediments from the Sea of Marmara. *Organic Geochemistry*, *85*, 42–53. https://doi.org/10.1016/j.orggeochem.2015.04.008
Bentaleb, I., Grimalt, J. O., Vidussi, F., Marty, J. C., Martin, V., Denis, M., et al. (1999). The C_{37} alkenone record of seawater temperature during seasonal thermocline stratification. *Marine Chemistry*, *64*, 301–313. https://doi.org/10.1016/s0304-4203(98)00079-6
Brassell, S. C., Eglinton, G., Marlowe, I. T., Pfaumann, U., & Sarnthein, M. (1986). Molecular stratigraphy: A new tool for climatic assessment. *Nature*, *320*, 129–133. https://doi.org/10.1038/320129a0
Cacho, I., Grimalt, J. O., Canals, M., Sbaffi, L., Shackleton, N. J., Schönfeld, J., & Zahn, R. (2001). Variability of the western Mediterranean Sea surface temperature during the last 25,000 years and its connection with the Northern Hemisphere climatic changes. *Paleoceanography*, *16*, 40–52. https://doi.org/10.1029/2000pa000502
Emeis, K. C., Struck, U., Schulz, H. M., Bernasconi, S., Sakamoto, T., Martinez-Ruiz, F., et al. (2000). Temperature and salinity of Mediterranean Sea surface waters over the last 16,000 years: Constraints on the physical environment of S1 sapropel formation based on stable oxygen isotopes and alkenone unsaturation ratios. *Palaeogeography, Palaeoclimatology, Palaeoecology*, *158*(3), 259–280. https://doi.org/10.1016/S0031-0182(00)00053-5
Locarnini, R. A., Mishonov, A., Antonov, J., Boyer, T., Garcia, H., & Levitus, S. (2006). *World Ocean Atlas 2005 Volume 1: Temperature [+DVD]* (p. 61). NOAA Atlas NESDIS.
Martrat, B., Grimalt, J. O., Lopez-Martinez, C., Cacho, I., Sierro, F. J., Flores, J. A., et al. (2004). Abrupt temperature changes in the western Mediterranean over the past 250,000 years. *Science*, *306*(5702), 1762–1765. https://doi.org/10.1126/science.1101706
Nieto-Moreno, V., Martínez-Ruiz, F., Willmott, V., García-Orellana, J., Masqué, P., & Sinninghe Damsté, J. S. (2013). Climate conditions in the westernmost Mediterranean over the last two millennia: An integrated biomarker approach. *Organic Geochemistry*, *55*, 1–10. https://doi.org/10.1016/j.orggeochem.2012.11.001
Rodrigo-Gámiz, M., Martínez-Ruiz, F., Rampen, S. W., Schouten, S., & Sinninghe Damsté, J. S. (2014). Sea surface temperature variations in the western Mediterranean Sea over the last 20 kyr: A dual-organic proxy (UK′37 and LDI) approach. *Paleoceanography*, *29*(2), 87–98. https://doi.org/10.1002/2013PA002466
Ternois, Y., Sicre, M.-A., Boireau, A., Conte, M., & E, G. (1997). Evaluation of long-chain alkenones as paleo-temperature indicators in the Mediterranean Sea. *Deep Sea Research Part I: Oceanographic Research Papers*, *44*(2), 271–286. https://doi.org/10.1016/s0967-0637(97)89915-3
Vidal, L., Menot, G., Joly, C., Bruneton, H., Rostek, F., Çağatay, M., et al. (2010). Hydrology in the Sea of Marmara during the last 23 ka: Implications for timing of Black Sea connections and sapropel deposition. *Paleoceanography*, *25*(1). https://doi.org/10.1029/2009pa001735
Zheng, Y., Heng, P., Conte, M. H., Vachula, R. S., & Huang, Y. (2019). Systematic chemotaxonomic profiling and novel paleotemperature indices based on alkenones and alkenoates: Potential for disentangling mixed species input. *Organic Geochemistry*, *128*, 26–41. https://doi.org/10.1016/j.orggeochem.2018.12.008